GE Nuclear Energy

COMMONWEALTH EDISON COMPANY
DRESDEN NUCLEAR POWER PLANT
UNITS 2 AND 3
SHROUD AND SHROUD REPAIR HARDWARE ANALYSIS
VOLUME I :
SHROUD REPAIR HARDWARE

Prepared by: Sofia Zaliznyak Date: 5/12/95
S. Zaliznyak, Engineer

for Date: _____
Y. Wu

Verified by: Date: 5/12/95
M. Kaul, Ph.D, Principal Engineer.

M.D. Potter for Date: 5/12/95
M. Wu

Approved by: Date: 5/12/95
K. Karim-Panahi, Ph.D., Principal Eng.

M.D. Potter Date: 5/12/95
M. Potter, Principal Engineer

A

ABSTRACT

Volumes I and II of this document provide the results of the stress analysis of the Dresden 2 and 3 and Shroud Repair Hardware, demonstrating that structural integrity is maintained when subjected to the loading and limits specified in Design Specification 25A5688.

EXECUTIVE SUMMARY

The volumes I and II of this report provides the results of the stress analysis of the Dresden Units shroud and shroud repair hardware when subjected to all applied loadings including seismic, pressure, deadweight, and thermal effects.

The shroud restraint hardware consists of four identical sets of tie rod and spring assemblies. The four sets are spaced 90° apart, beginning at 20° from vessel zero. Each set consists of the following major elements:

1. An Upper Spring, located in the reactor pressure vessel (RPV)/shroud annulus at the top guide elevation. This spring provides lateral seismic support to the shroud at the top guide elevation and transmits seismic loads from the nuclear core directly to the RPV.

2. An Upper Support Assembly, located in the annulus from the top guide elevation to the top of the shroud. This assembly provides a connection for the tie rod to the shroud top.

3. A Middle Spring, located in the annulus at the elevation of the jet pump support brackets. This spring provides lateral seismic support to the shroud, keeps the shroud from coming in contact with the jet pump support brackets during a seismic event, and restrains the tie rod movement for proper tie rod vibration characteristics.

4. A Lower Spring, located in the annulus at the core plate and shroud support region. This spring provides lateral seismic support to the shroud, transmitting core seismic loads to the RPV. In addition, this spring provides a connection for the tie rod to the shroud support plate.

5. The Tie Rod, which connects to the upper end of the top of the shroud and to the lower end of the lower spring. This component develops a thermal preload due to normal operating temperature, which in turn provides vertical clamping forces to the shroud.

The upper, middle and lower springs are optimized to transfer the lateral operational, hydrodynamic and seismic loads while meeting the stress limits.

The stress analysis of the overall core shroud was performed with the ANSYS code [Reference 1]. A three-dimensional finite element model was constructed which included the shroud from the upper flange at the shroud head joint down to the connections at the RPV. Because of the symmetrical behavior of the shroud under the applied loads, a 180° circumferential segment was modeled.

The stress analysis of the major shroud repair hardware components was performed with the COSMOSM [Reference 10] and ANSYS codes. For the smaller components, hand calculations were performed.

The load combinations and structural acceptance criteria are contained in the Design Specification [Reference 2]. The results of the stress analysis demonstrate that the shroud and shroud repair hardware meet the requirements of that specification.

The Volume I of this report is describing the analysis of the shroud repair hardware.

IMPORTANT NOTICE REGARDING THE CONTENTS OF THIS REPORT

The only undertaking of the General Electric Nuclear Energy (GENE) respecting information in this document are contained in the contract between Commonwealth Edison (ComEd) and GENE, and nothing contained in this document shall be construed as changing this contract. The use of this information by anyone other than ComEd, or for any purpose other than that for which it is intended, is not authorized; and with respect to any unauthorized use, GENE makes no representation or warranty and assumes no liability as to the completeness, accuracy, or usefulness of the information contained in this document.

Table of Contents

List of Figures

COMMONWEALTH EDISON COMPANY
DRESDEN NUCLEAR POWER PLANT
UNITS 2 AND 3
SHROUD AND SHROUD REPAIR HARDWARE ANALYSIS
VOLUME I :
SHROUD REPAIR HARDWARE

1.0 INTRODUCTION

Intergranular stress corrosion cracking (IGSCC) has been found in the core shroud welded joints of several Boiling Water Reactors. Similar cracking may also exist in the welded joints of the Dresden Units 2 and 3 Core Shroud. GENE has designed a shroud repair system that reinforces the shroud in the event that any or all of the seven shroud horizontal weld joints are cracked. The stress analysis discussed in this report demonstrates that the shroud and the shroud repair system structural integrity is maintained if any or all of these seven welded joints are cracked completely through their thickness and around their entire 360° circumference. The structural integrity of the shroud and shroud repair system is also demonstrated in the event that the shroud is uncracked and the repair system is installed.

The Volume I of this report is describing the analysis of the shroud repair hardware.

2.0 SHROUD REPAIR SYSTEM DESIGN FEATURES

The shroud repair system consists of four identical sets of tie rod and spring assemblies. The four sets are spaced at 90° intervals beginning at 20° from vessel zero. A layout of one of the tie rod and spring sets is shown in Figure 2.1.

The tie rods are thermally preloaded to provide vertical compressive clamping forces on the shroud. The magnitude of the tie rod thermal preload is greater than the net uplift forces on the shroud due to normal operating pressures and postulated Loss of Coolant Accident (LOCA) recirculation line break pressures, so that no vertical separation of shroud sections would occur in those cases if the welded joints are postulated to be completely cracked. This is not the case for postulated LOCA main steam line break uplift pressures, which are sufficient to overcome the tie rod preload and momentarily separate shroud sections.

The upper, middle, and lower springs provide a lateral seismic load path from the top guide and core plate to the RPV. The magnitude of the seismic loads in these springs is a function of their stiffness. The stiffness has been optimized to minimize the seismic loads while still meeting the stress and displacements limits. The U-shaped upper springs consists of tapered legs that flex towards each other under lateral seismic loads. The taper in these legs has been optimized to produce constant stress along their length while providing the required stiffness. For the middle spring, the flexibility of the taper beam section provides the needed lateral stiffness to keep the middle section of the shroud from coming in contact with the jet pump support brackets during a seismic event. This keeps the shroud from moving closer than 1/2-inch to the jet pump support bracket. The rigid middle section of the middle spring also provides an intermediate lateral support to the tie rod. The natural vibration frequency of the tie rod with this intermediate support is then well removed from the flow-induced forcing frequency (flow induced vibration is discussed in detail in Section 6.6). For the lower spring, the flexibility of the Y-shaped feature at the top provides the lateral stiffness property, whereas the flexibility of the straight middle section provides the axial stiffness property, which in combination with the stiffness of the tie rod and upper axial component determines the tie rod thermal preload.

The shroud geometry and location and designation of the seven shroud horizontal weld joints are shown in Figure 2.2.

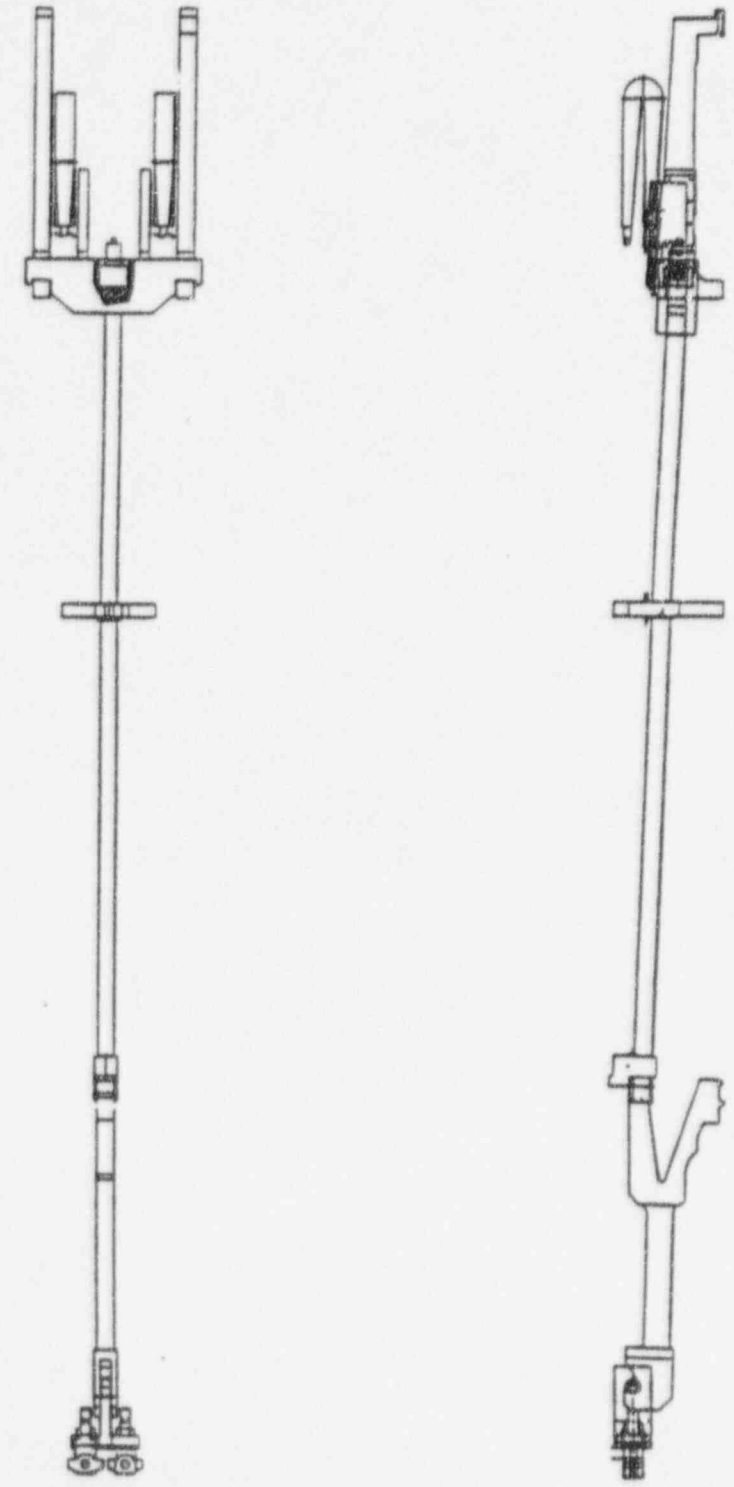

Figure 2.1 Shroud Repair Hardware Layout

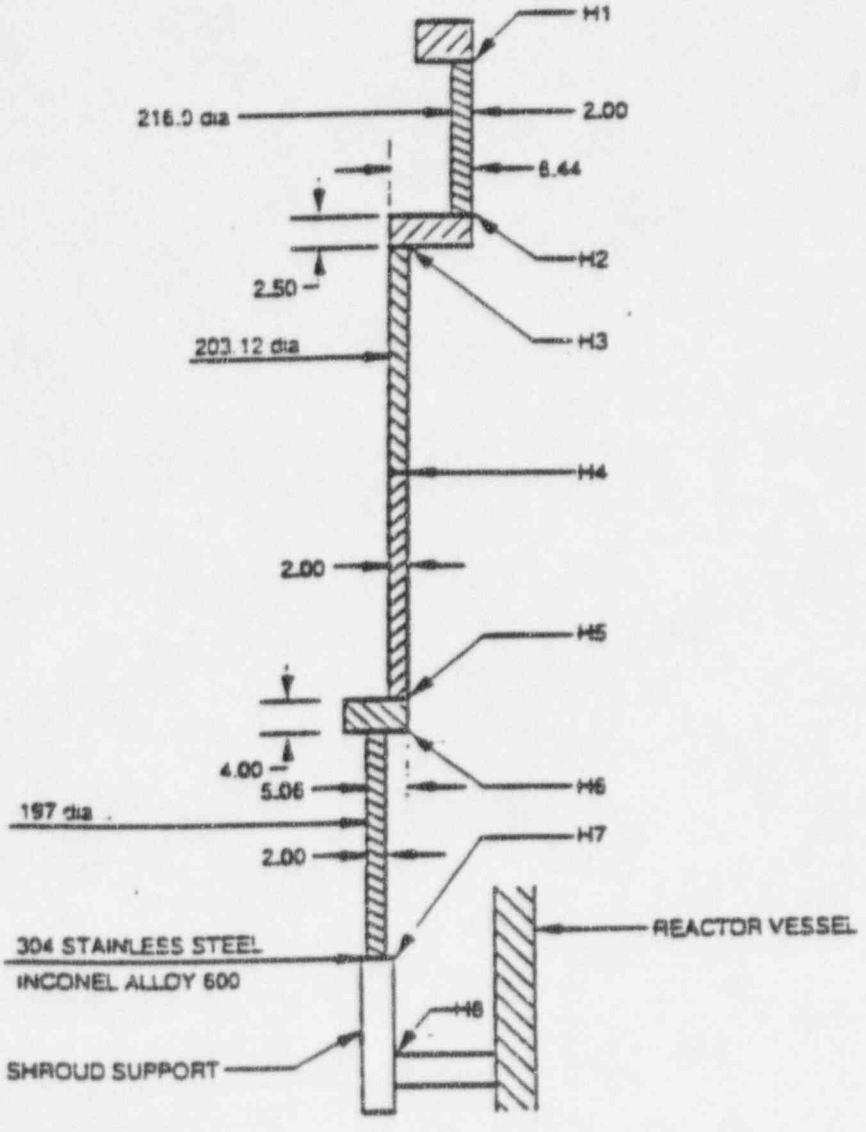

Figure 2.2 Shroud Horizontal Weld Designations

3.0 MATERIAL PROPERTIES

The following material properties for the primary load bearing restraint components are taken from Appendix I of the ASME B&PV Code [Reference 3] and GENE Testing Report [Reference 4]. A 575° F temperature applies to the Normal and Upset condition, and a 550° F temperature applies to the Faulted and Emergency conditions.

3.1 **Tie Rod** (Drawing 112D6672)

XM-19	at 550° F (oper.)	
Young's Modulus	25.6 E6 psi	Table I-6 [Reference 3]
Thermal Expansion Coefficient	8.98 E-6 in/in/°F	Table I-5 [Reference 3]
S_m	29450 psi	Table I-1.2 [Reference 3]
$S_{p.l.}$*	31440 psi**	Table I-2.2 [Reference 3]

* The proportional limit for the material is 80 percent of the yield strength.

** This is the $S_{p.l.}$ at 300°F.

3.2 **Spring and Upper Assemblies** (Upper Spring Drawing 112D6670; Long Upper Support Drawing 112D6669, Bracket Drawing 112D6675; Middle Spring Drawing 112D6681; and Lower Spring Drawing 112D6671)

X-750	at 550° F (oper.)	
Young's Modulus	28.4 E6 psi	[Reference 4]
Thermal Expansion Coefficient	7.5 E-6 in/in/ °F	[Reference 4]
S_m	47500 psi	[Reference 4]
$S_{p.l.}$	74560 psi	[Reference 4]

4.0 LOADS AND LOAD COMBINATIONS

The Design Specification [Reference 2] specifies that the shroud and shroud repair hardware shall be analyzed for the following load combinations:

Normal / Upset	ΔP_N + DW + OBE
Emergency 1	ΔP_N + DW + DBE
Emergency 2	$\Delta P_{MS\text{-}LOCA}$ + DW
Emergency 3	$\Delta P_{RC\text{-}LOCA}$ + DW
Faulted 1	$\Delta P_{MS\text{-}LOCA}$ + DW + DBE
Faulted 2	$\Delta P_{RC\text{-}LOCA}$ + DW + DBE

where: ΔP_N = Normal Pressure Difference
DW = Dead Weight Loads
OBE = Operating Basis Earthquake
DBE = Design Basis Earthquake
$\Delta P_{MS\text{-}LOCA}$ = Main Steam Line LOCA
$\Delta P_{RC\text{-}LOCA}$ = Recirculation Line LOCA
LOCA = Loss of Coolant Accident

The OBE and DBE loads are reported in Reference [5]. Since the configuration of the seismic model depends on the assumed behavior at weld joints postulated to be cracked, and the resulting seismic loads depend on this assumed behavior, two sets of DBE seismic loads were established. One set corresponds to the configuration for normal pressure differences and was used in the Emergency 1 load combination. The second set of seismic loads corresponds to the configuration for Main Steam Line LOCA pressure differences and was used in the Faulted 1 load combination. The configuration of the seismic model for the recirculation line outlet LOCA corresponds to that for normal pressure differences, and hence the seismic loads to be combined in the Faulted 2 load combination for the recirculation line outlet LOCA are from the first set of loads.

After reviewing the FSAR, it was determined that the shroud loads due to a feedwater line break are bounded by the main steam line break loadings and the recirculation line break loadings.

The appropriate deadweight loads were used in this stress analysis. The effect of the vertical seismic accelerations on the deadweight were also included.

The pressure difference loads are taken from the Design Specification [Reference 2].

5.0 STRUCTURAL ACCEPTANCE CRITERIA

The Design Specification specifies the following stress intensity limits in the Repair Hardware.

	Resulting Stress			S_{allow}
Upset	Primary Membrane	P_m	<	1.00 x S_m
	Primary Membrane + Primary Bending	$P_m + P_b$	<	1.50 x S_m
Emergency	Primary Membrane	P_m	<	1.50 x S_m
	Primary Membrane + Primary Bending	$P_m + P_b$	<	2.25 x S_m
Faulted	Primary Membrane	P_m	<	2.00 x S_m
	Primary Membrane + Primary Bending	$P_m + P_b$	<	3.00 x S_m
Thermal Upset	Primary Membrane + Primary Bending + Secondary	$P_m + P_b + Q$	<	3.00 x S_m

For the evaluation of lower springs under Alternate Normal / Upset and Thermal Upset conditions, the maximum stress will be limited to the proportionality limit, i.e., 0.8 x S_y.

6.0 SHROUD REPAIR HARDWARE STRESS ANALYSIS

The shroud repair hardware, i.e. the tie rod system, provides axial stiffness and thermally-induced shroud hold-down forces. The tie rod system, as shown in Figure 2.1, includes: the Tie Rod (Drawing 112D6640), the Upper Spring and Support Assembly (Drawing 112D6641), the Middle Spring (Drawing 112D6680), and the Lower Spring and Support Assembly (Drawing 112D6638). The axial stiffness of these components act in series creating a total tie rod system stiffness of 650 kips/inch, which is very close to the value used in the seismic analysis (609 kips/inch). The upper supports and lower spring stiffness values were obtained from the finite element analyses discussed below.

Two steady state thermal conditions are identified in the design specification. The first is Normal operation with the shroud at 550^{O} F and the tie rod system at 538^{O} F. The second is an Upset condition with the shroud at 433^{O} F and the tie rod system at 300 F. Using the 609 kips/inch system stiffness and the appropriate dimensional and thermal expansion values, the tie rod system axial thermal preloads corresponding to these two thermal conditions are given in Ref. [11].

The tie rod net load is a combination of the thermal preload, seismic load, and the effect of the net uplift force from the shroud head due to pressure difference and deadweight. For the upset and emergency load combinations, the thermal preload is not overcome and the shroud has a compressive clamping force. In this case, the tie rod load due to the shroud head net uplift force is proportional to the relative stiffness of the tie rod versus the shroud, as in a preloaded bolted joint. For the faulted combination with Main Steam Line LOCA and RRLB, the preload is overcome and the net shroud head uplift force is reacted by the tie rods. The maximum tie rod tensile loads for the load combinations were derived on that basis, and have the following magnitudes [Ref. 12]:

Case	F (kips)
Upset with OBE	194.00
Upset Thermal	170.00
Emergency	339.00
Faulted	339.00

Since the number of applied load cycles for upset/OBE, emergency and faulted cases is very small, no formal fatigue analysis is required for the shroud repair hardware. As for the Normal/Upset case, the resulting stress is relatively low, and the allowable number of fatigue cycles is high. Therefore only the tie rod fatigue is analyzed for thermal upset condition is addressed in Section 6.6.

6.1 Shroud Upper Stabilizer

6.1.1. INTRODUCTION

This section summarizes the results of the stress analysis performed on upper spring of the shroud repair hardware for Dresden 2 and 3 Project

This spring (stabilizer) is part of tie rod assembly and provides lateral seismic support to the shroud and transmits seismic loads from the nuclear core directly to the RPV. Normal/Upset, Emergency and Faulted conditions, that include seismic, pressure, gravity and thermal loads, were analyzed and the maximum stresses were shown to be within the allowable limits.

In addition the results of the analysis were used to compute stiffness constants for the Spring for use in global shroud model.

6.1.2. ANALYSIS METHOD

Detailed finite element model of the spring was constructed to evaluate the upper stabilizer's mechanical characteristics and stresses. The model was built in detail and analyzed for different loading conditions using the static analysis option of the COSMOS finite element code [Ref.10]. The code is developed by Structural Research and Analysis Corporation (SRAC) of Los Angeles California. It has been verified for use in the nuclear power industry per the requirements of 10CFR50 Appendix B and the applicable section of ANSI/ASME QA-1 and related supplements.

6.1.3. MATERIAL PROPERTIES AND APPLIED LOADS

The upper spring is made of INCONEL X-750 material, for which the material properties have been tabulated below.

TABLE 6.1-1: Upper Spring Material Properties

Property	Description	Value
ρ	Density	0.29 lb/in^3
E	Modulus of Elasticity	28.4 x 10^6 psi
μ	Poisson's ratio	0.3

Applied loads for different conditions and corresponding allowable stresses are shown in the following table.

TABLE 6.1-2: Upper Spring Applied Side Loads and Allowable Stresses

Identification	Condition	Applied loads (lb.)	Allowable Stress Pm+Pb,(psi)
Upper Spring	Normal/Upset Emergency Faulted	33,500 67,000 70,000	70,500 106,875 142,500

6.1.4. MODELING DETAILS

The shroud upper spring located in the reactor pressure vessel (RPV) shroud annulus at the top guide elevation. This spring provides lateral seismic support to the shroud at the top guide elevation and transmits seismic loads from the nuclear core directly to RPV. To evaluate the accurate linear spring constant and stress values, a finite element model was made with solid elements. Figure 6.1-1 depicts the meshing of this spring, applied loads and boundary condition. Figure 6.1-2 through 6 show the distribution of stress and displacements under Normal/Upset, Emergency and Faulted condition. The upper spring's linear spring constant extracted from the detailed model is used in the global model to represent the spring. To calculate the proper actual maximum stresses, the maximum stresses extracted from this model are prorated with actual loads extracted from the global model.

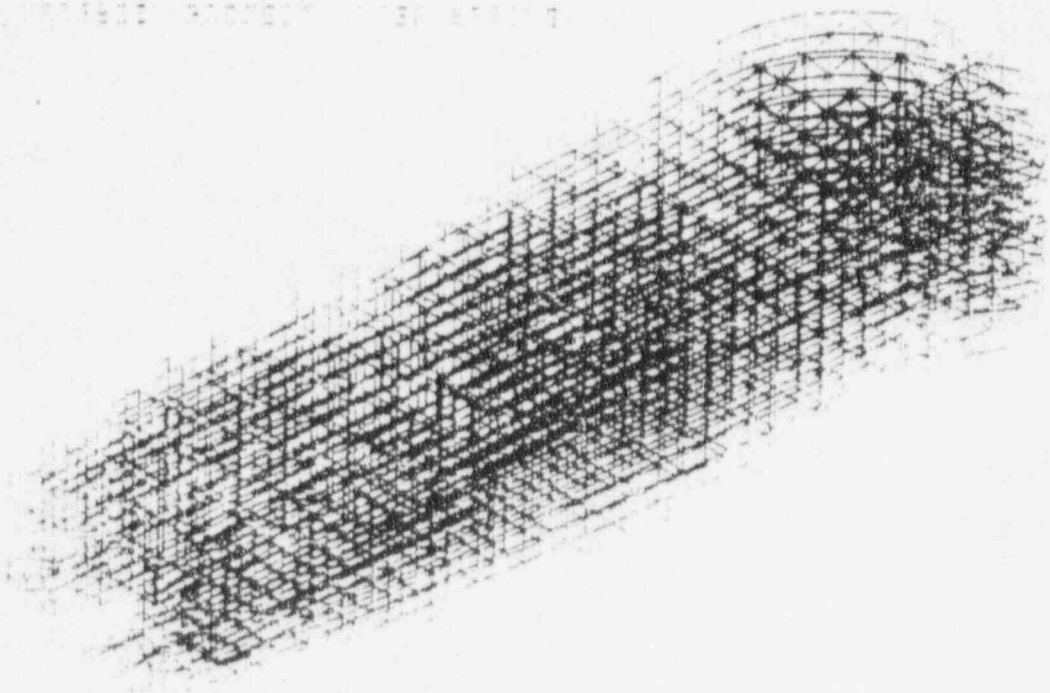

Figure 6.1-1 Upper Spring Finite Element Model

6.1.5. ANALYSIS RESULTS

The table below shows the shroud upper spring stresses during Normal/Upset and emergency and faulted events .

TABLE 6.1-3: Upper Spring Stress Summary

Condition	**Applied loads (lbs)**	Stress Intensity **(psi)**	**Allowable stress (Pm+Pb)(psi)**
Normal/Upset	33500	51,800	70,500
Emergency	67000	103,600	106,875
Faulted	70000	108,200	142,500

As is seen in Table 6.1-3 all stresses for the critical load combinations are below the corresponding allowables.

6.1.6. SPRING CONSTANT

Based on the results of the finite element model of the upper spring the following spring constants are calculated:

Horizontal spring constant: 62 kips/in

The local axial shroud flexibility is negligible in comparison to the upper spring flexibility. Therefore the effect of the shroud axial flexibility is neglected in the calculation of the above spring constant.

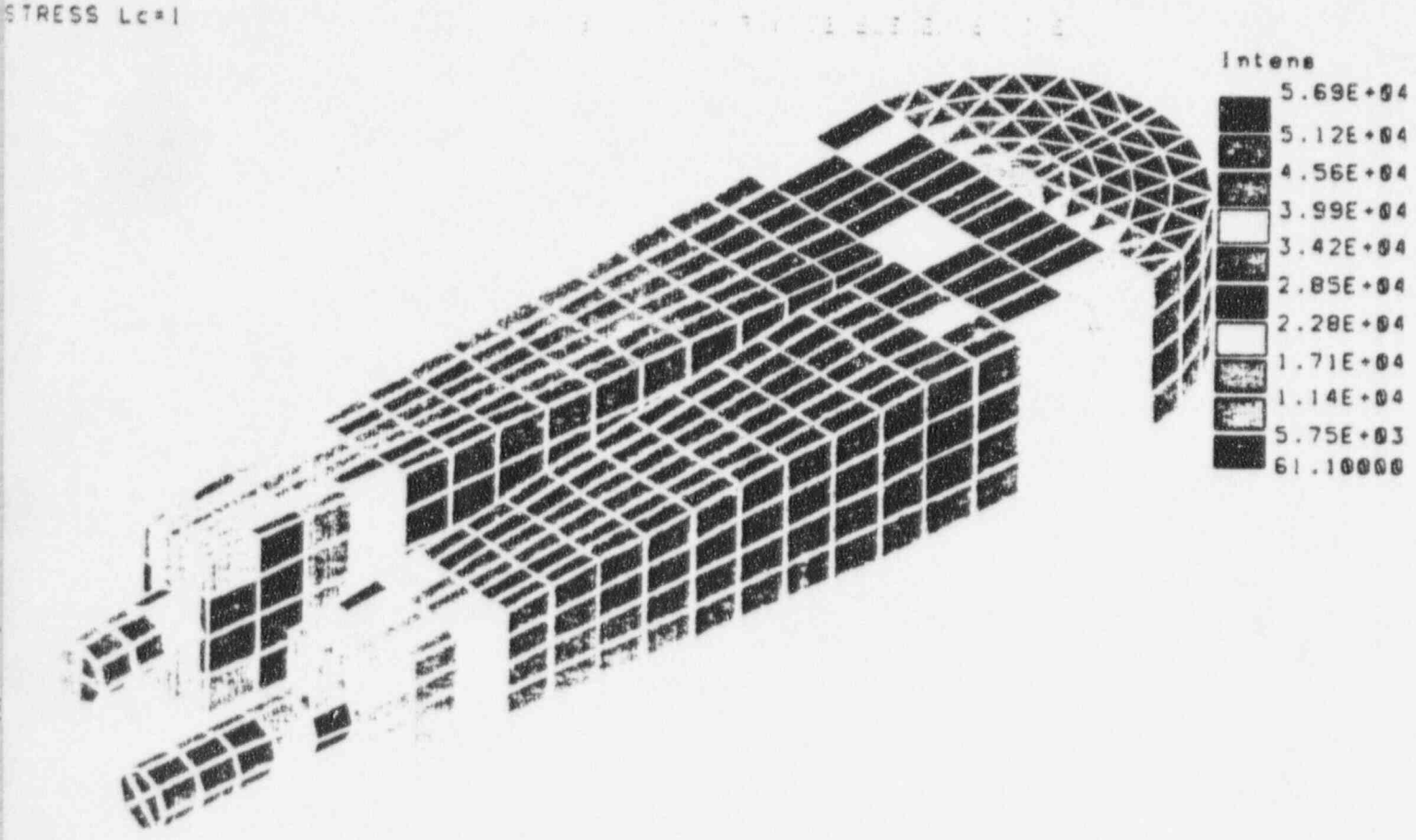

Figure 6.1-2 Upper Spring Normal/Upset Condition, Stress Intensity

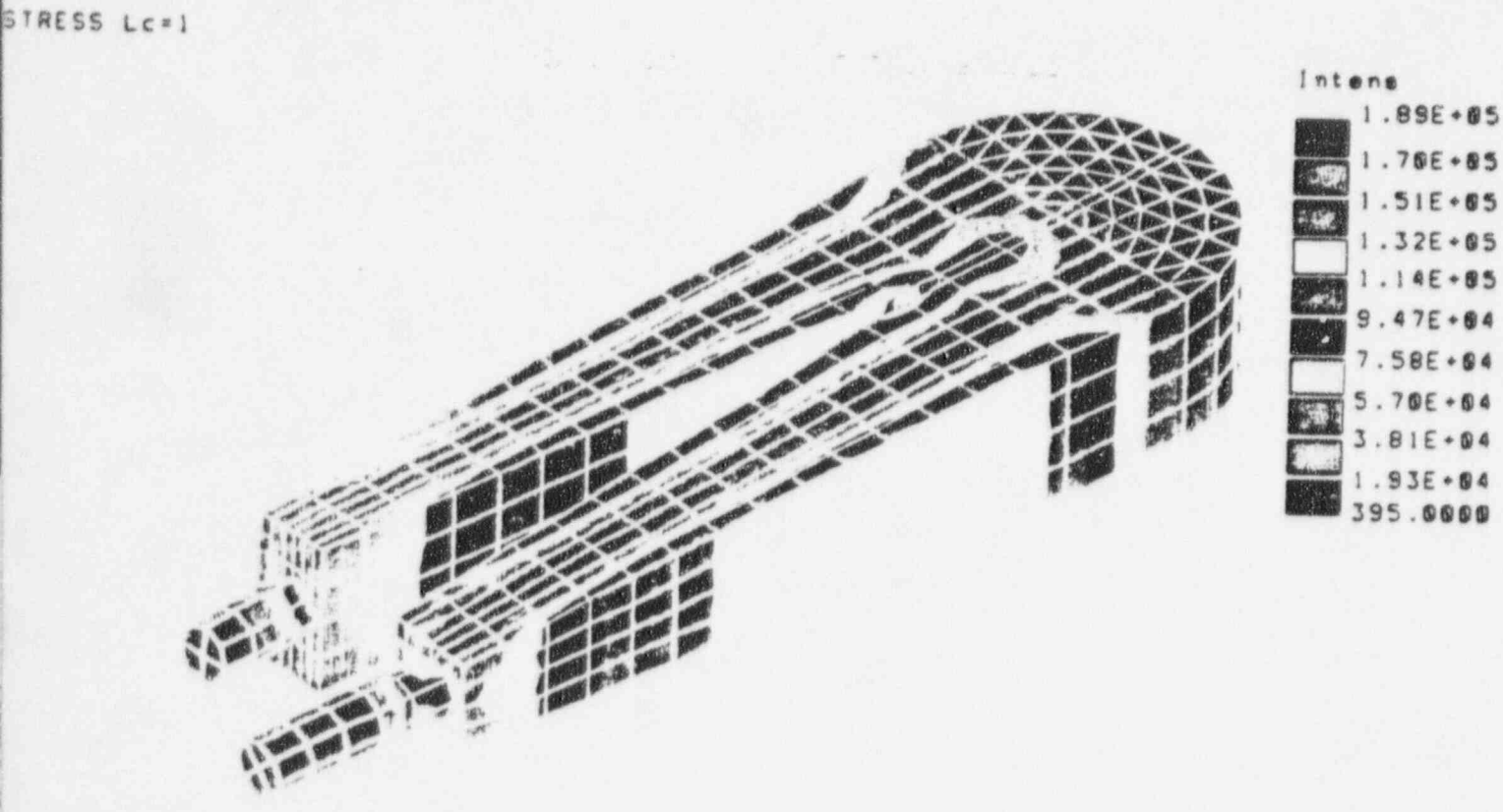

Figure 6.1-3 Upper Spring Emergency Condition, Stress Intensity

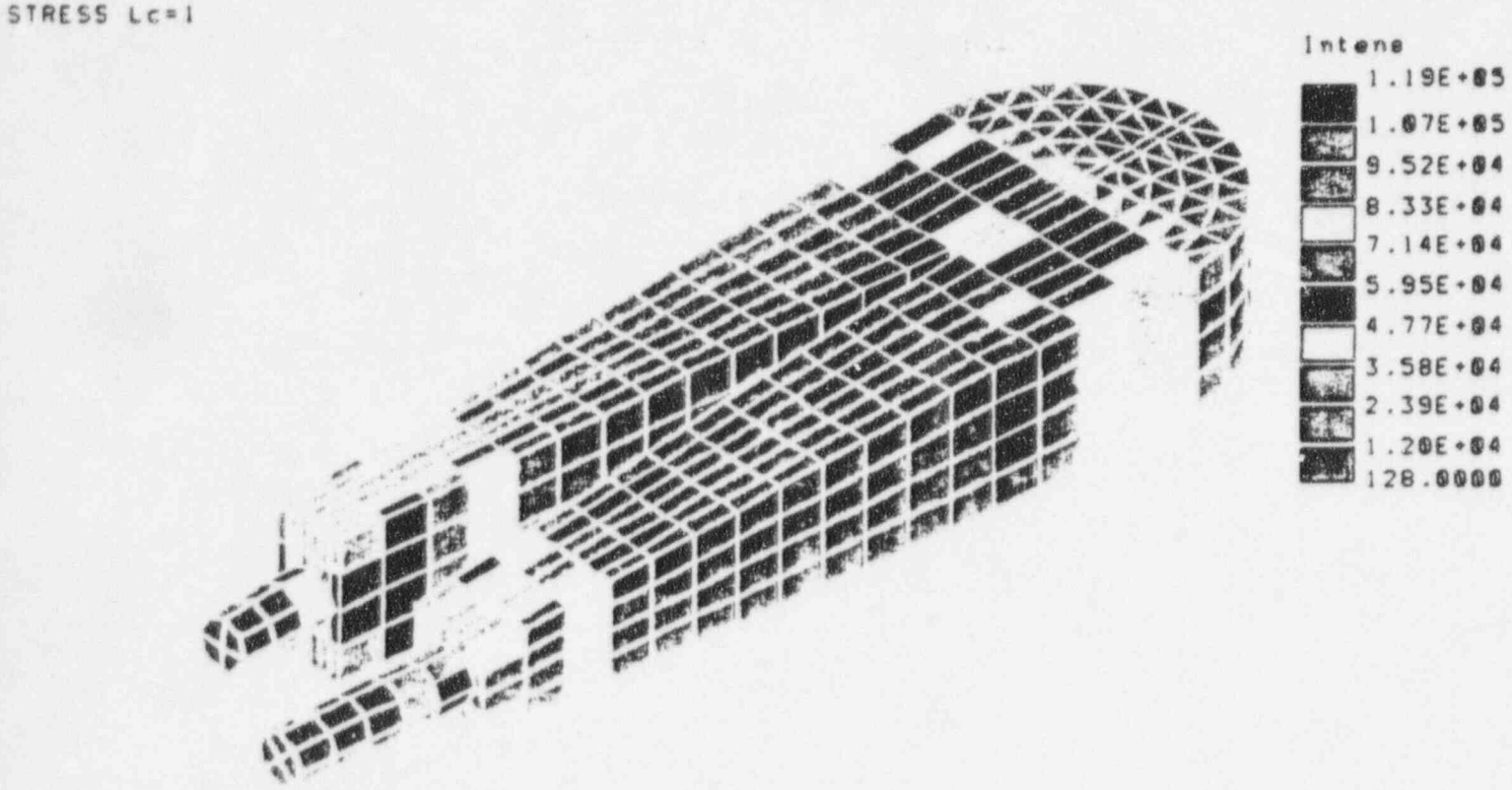

Figure 6.1-4 Upper Spring Faulted Condition, Stress Intensity

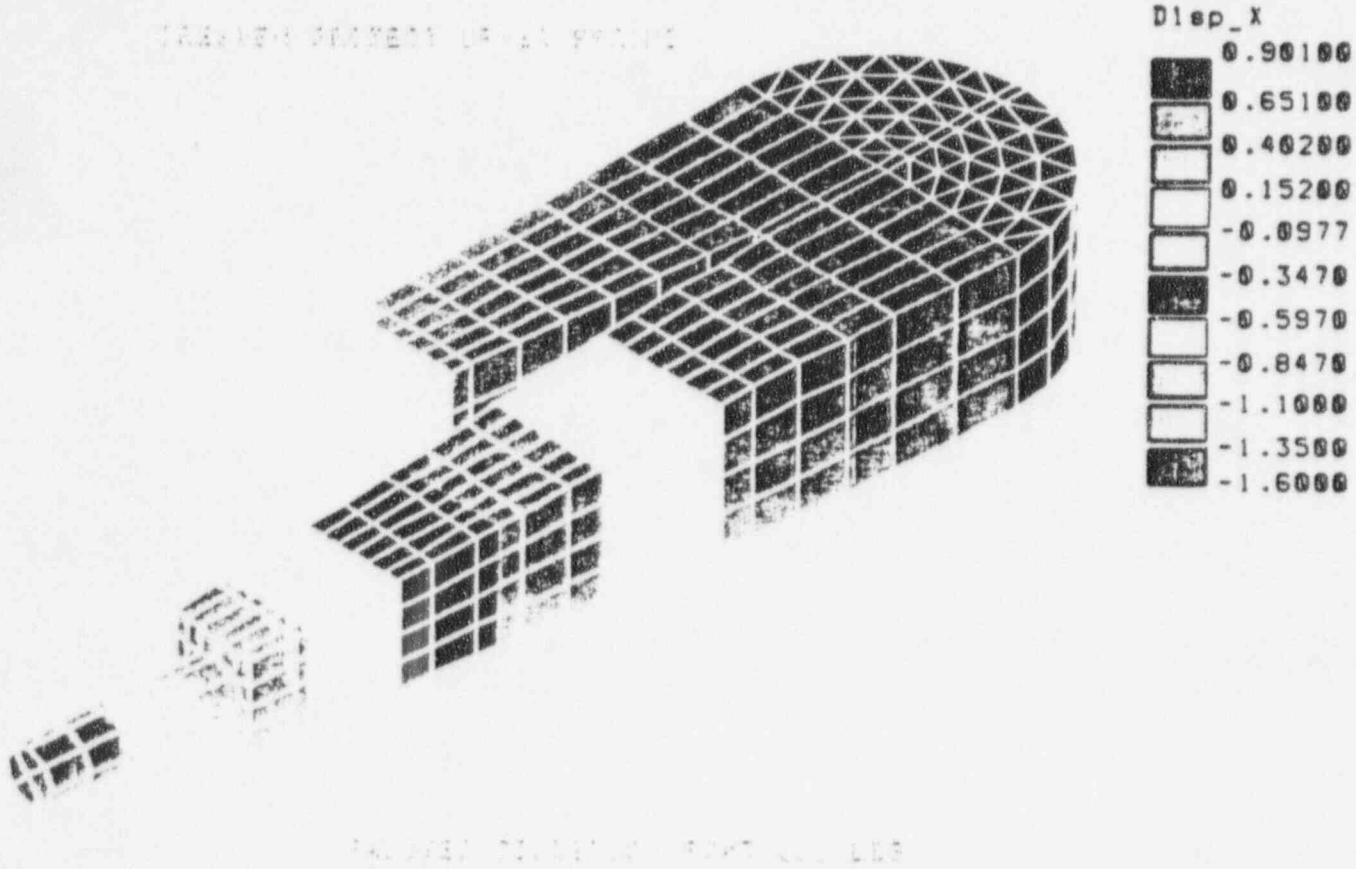

Figure 6.1-5 Upper Spring Faulted Condition, Displacement

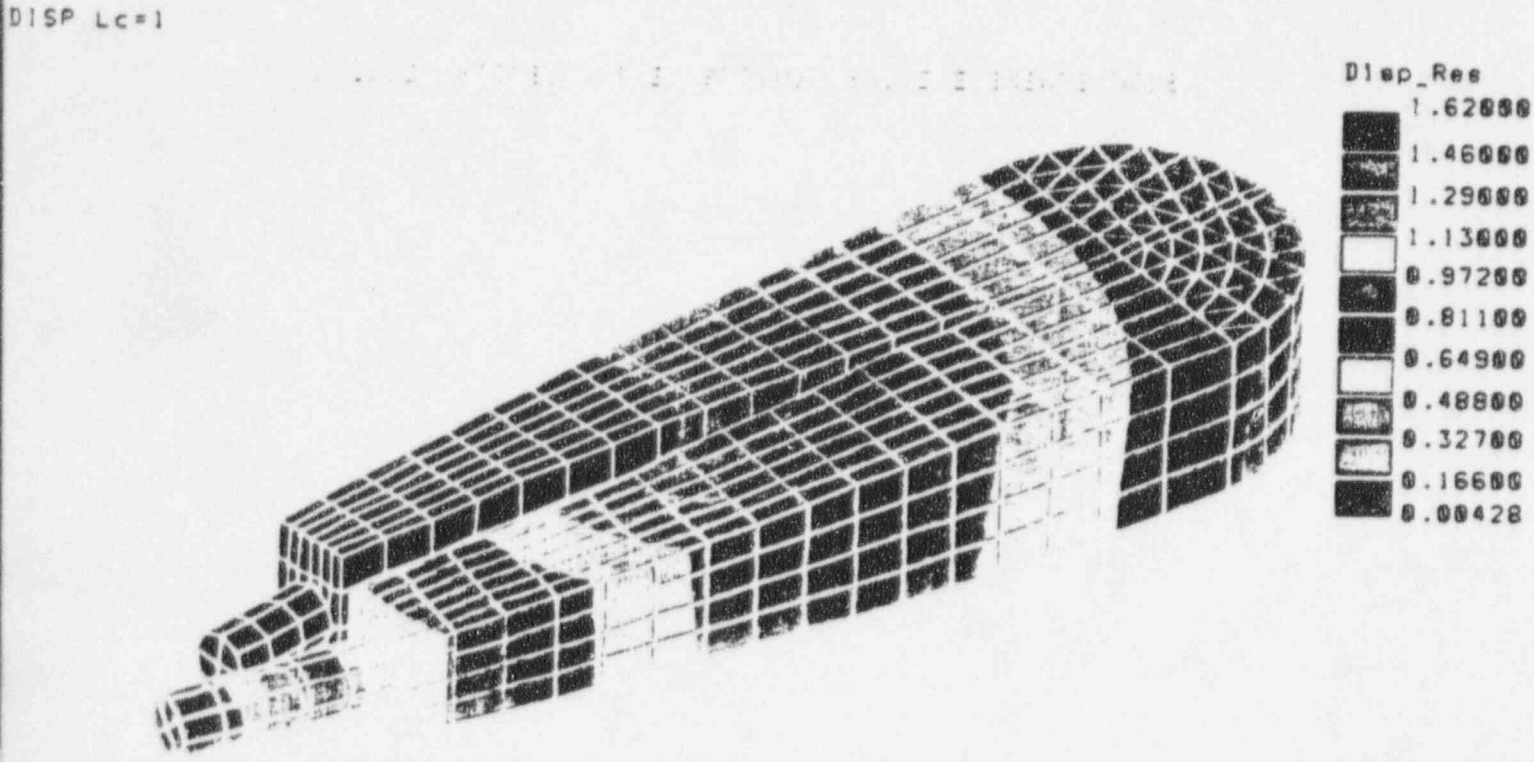

Figure 6.1-6 Upper Spring Faulted Condition, Deformation (Magnified)

6.2 Shroud Lower Stabilizer

6.2.1. INTRODUCTION

This section summarizes the results of the stress analysis performed on lower spring of the shroud repair hardware for Dresden 2 and 3 Project. This spring (stabilizer) is part of tie rod assembly and provides lateral seismic support to the shroud and transmits seismic loads from the nuclear core directly to the RPV. Normal/Upset, Emergency and Faulted conditions, that include seismic, pressure, gravity and thermal loads, were analyzed and the maximum stresses were shown to be within the allowable limits.

In addition the results of the analysis were used to compute stiffness constants for the Spring for use in global shroud model.

6.2.2. ANALYSIS METHOD

Detailed finite element model of the spring was constructed to evaluate the lower stabilizer's mechanical characteristics and stresses. The model was built in detail and analyzed for different loading conditions using the static analysis option of the COSMOS finite element code. The code is developed by Structural Research and Analysis Corporation (SRAC) of Los Angeles California. It has been verified for use in the nuclear power industry per the requirements of 10CFR50 Appendix B and the applicable section of ANSI/ASME QA-1 and related supplements.

6.2.3. MATERIAL PROPERTIES AND APPLIED LOADS

The lower springs is made of INCONEL X-750 material, for which the material properties have been tabulated below.

TABLE 6.2-1: Lower Spring Material Properties

Property	Description	Value
ρ	Density	0.29 lb/in^3
E	Modulus of Elasticity	28.4 x 10^6 psi
μ	Poisson's ratio	0.3

Applied loads for different conditions and corresponding allowable stresses are shown in the Table 6.2-2.

TABLE 6.2-2: Lower Spring Applied loads and Allowable Stresses

Identification	Condition (*)	Applied loads (lb.)	Allowable Stress (Pm+Pb)(psi)
LOWER SPRING	Normal / Upset:		
	Side Load	93,000	70,500
	Vert. Load	194,000	70,500
	Emerg.: Side Load	186,000	106,875
	Vert. Load	339,000	106,875
	Faulted: Side Load	190,000	142,500
	Vert. Load	339,000	142,500

* Vertical and side loads do not act simultaneously on the same spring.

6.2.4. MODELING DETAILS

The shroud lower spring, located in the annulus at the core plate and shroud support region. This spring consists of a diapason-like structure with the fork handle on a simple support, and provides lateral seismic loads to the RPV. In addition this spring provides a connection for the tie rod to the shroud support plate. To evaluate the accurate linear spring constant and stress values, a finite element model was made with solid elements. Figure 6.2-1 depicts the meshing of this spring, applied loads and boundary condition. The model is assumed hinged at the support locations and loads shown above were applied at the location of contact with shroud and tie rod. Figures 6.2-2 through 6.2-6 show distribution of stress and displacements under Normal/Upset , Emergency and Faulted condition . The lower spring's linear spring constant, extracted from the detailed model, is used in the global model to represent this spring.

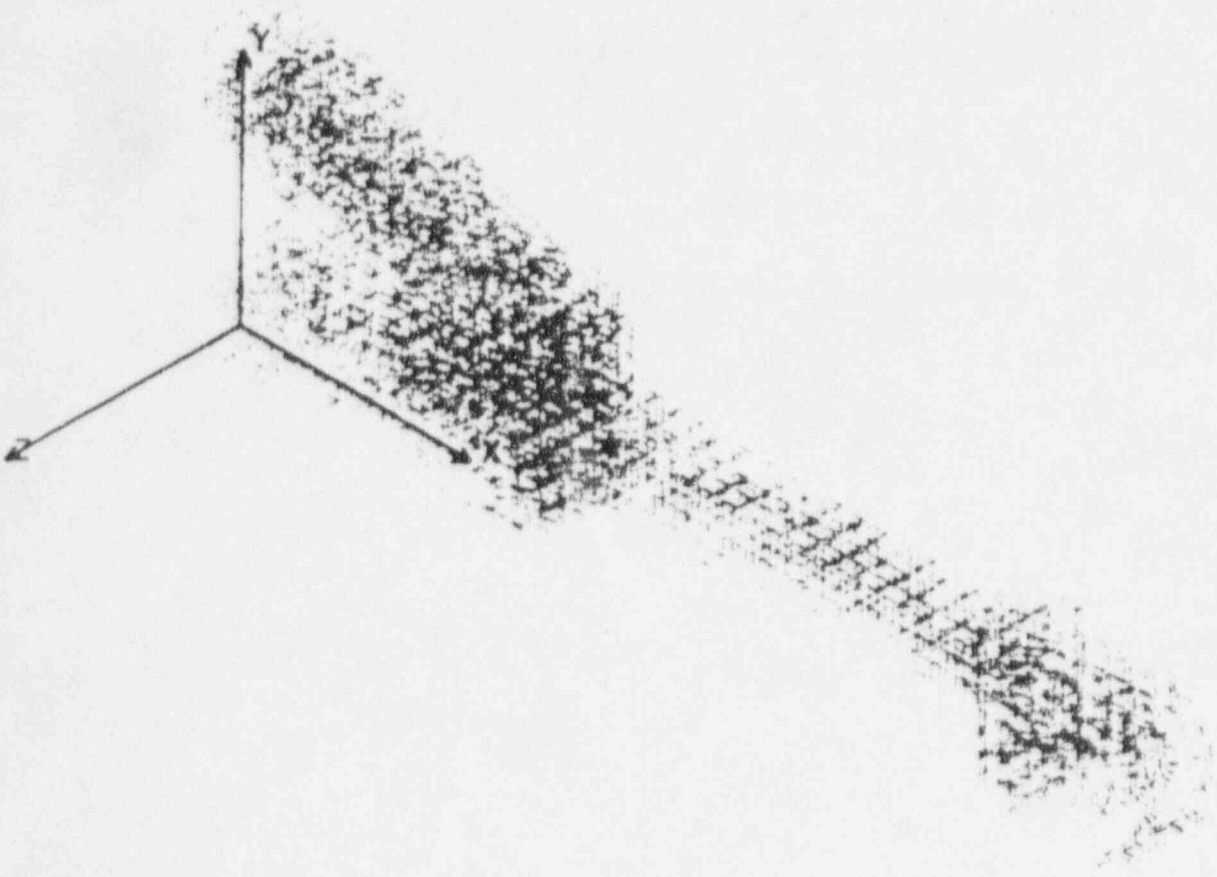

Figure 6.2-1 Lower Spring Finite Element Model

6.2.5. ANALYSIS RESULTS

The table below shows the shroud lower spring stresses during Normal/Upset and emergency and faulted events .

TABLE 6.2-3: Lower Spring Stress Summary

Condition	Applied loads (lbs)		Stress Intensity (psi)	Allowable stress (psi)
Normal / Upset	Side Load Vert. Load	93000 194000	43400 59500	70,500 70,500
Emergency	Side Load Vert. Load	186000 339000	86800 104000	106,875 106,875
Faulted	Side Load Vert. Load	190000 339000	88700 104000	142,500 142,500

As is seen in Table 6.2-3, all stresses for the critical load combinations are below the corresponding allowables.

6.2.6. SPRING CONSTANT

Based on the results of the finite element model of the lower spring the following spring constants are calculated:

Transverse spring constant: 325 kips/in

This spring constant includes the local flexibilities of shroud and RPV. The spring constant used in the seismic analysis is 300 kips/in which is 7.69% different from the calculated value, which is an acceptable difference.

Axial spring constant: 1973 kips/in

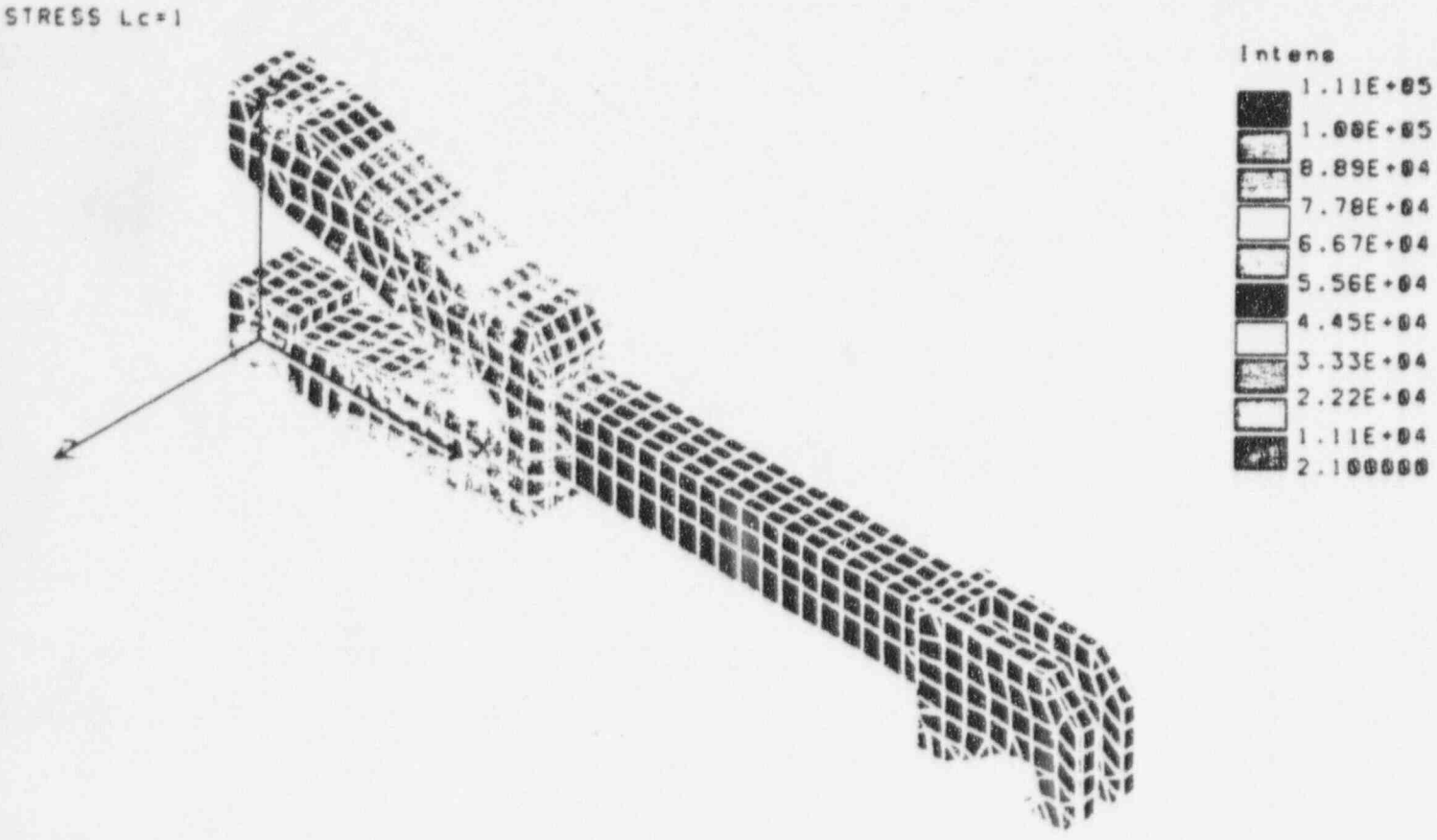

Figure 6.2-2 Lower Spring Normal/Upset Condition, Stress Intensity

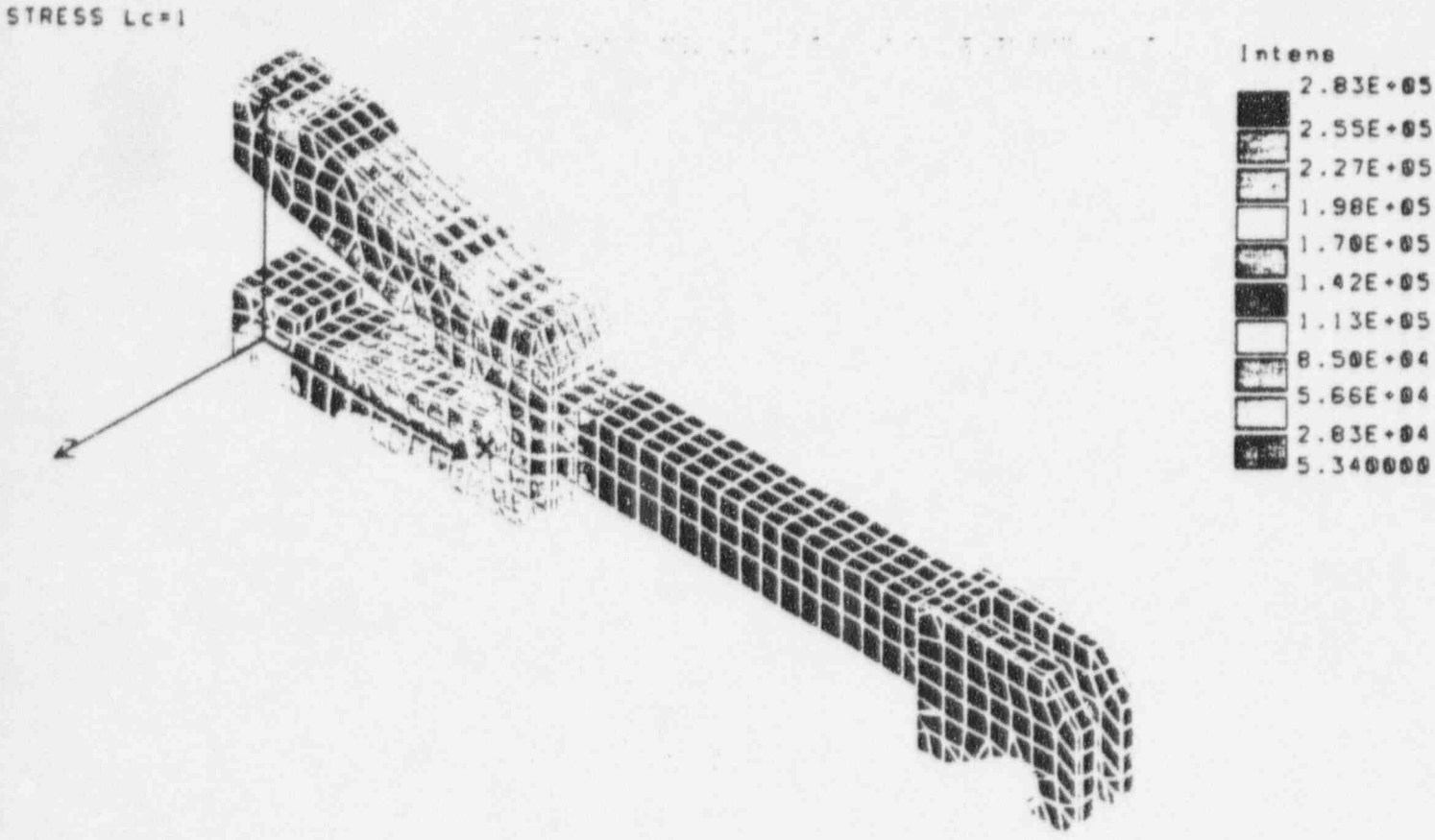

Figure 6.2-3 Lower Spring Emergency Condition, Stress Intensity

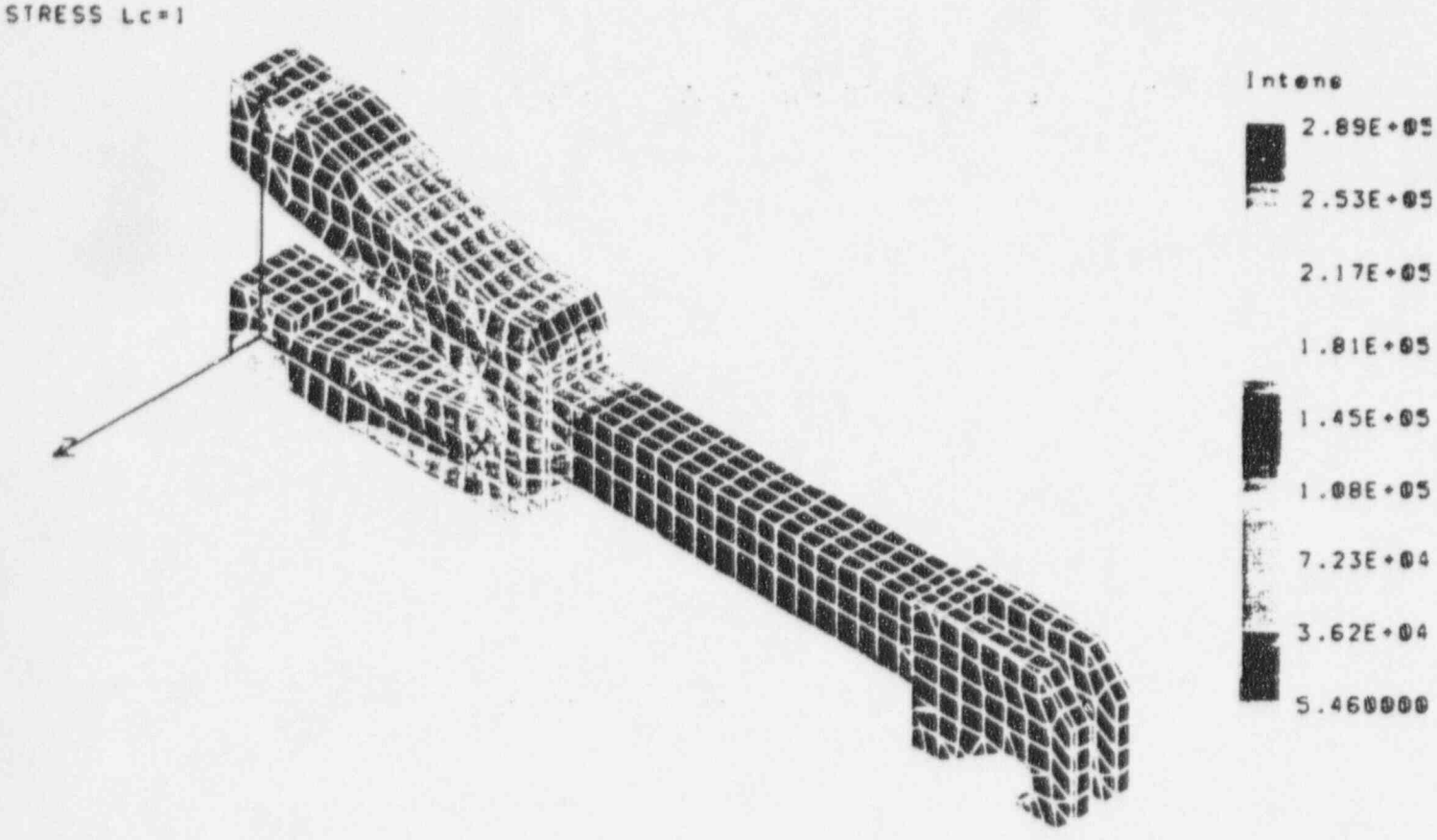

Figure 6.2-4 Lower Spring Faulted Condition, Stress Intensity

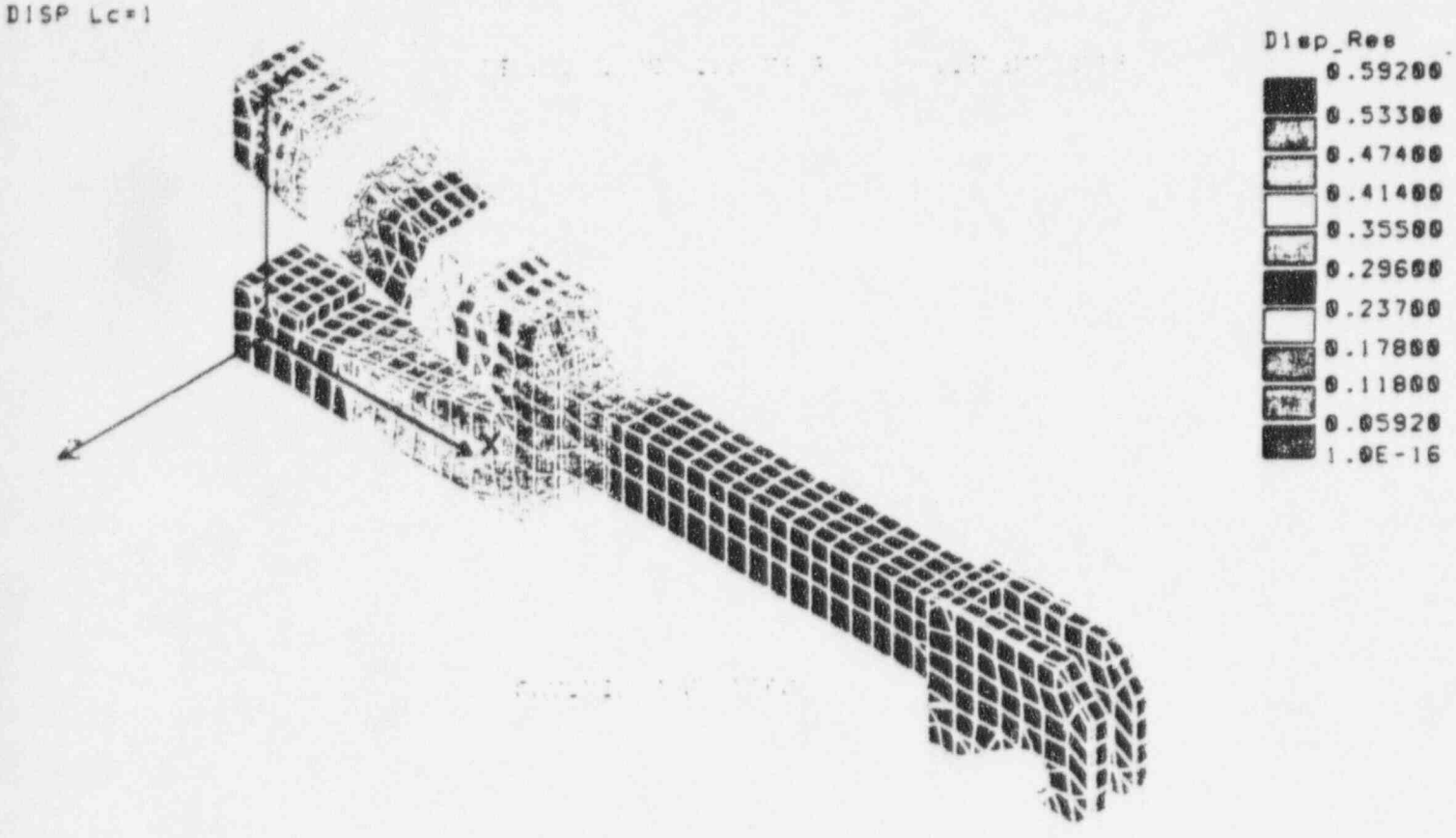

Figure 6.2-5 Lower Spring Faulted Condition, Displacement

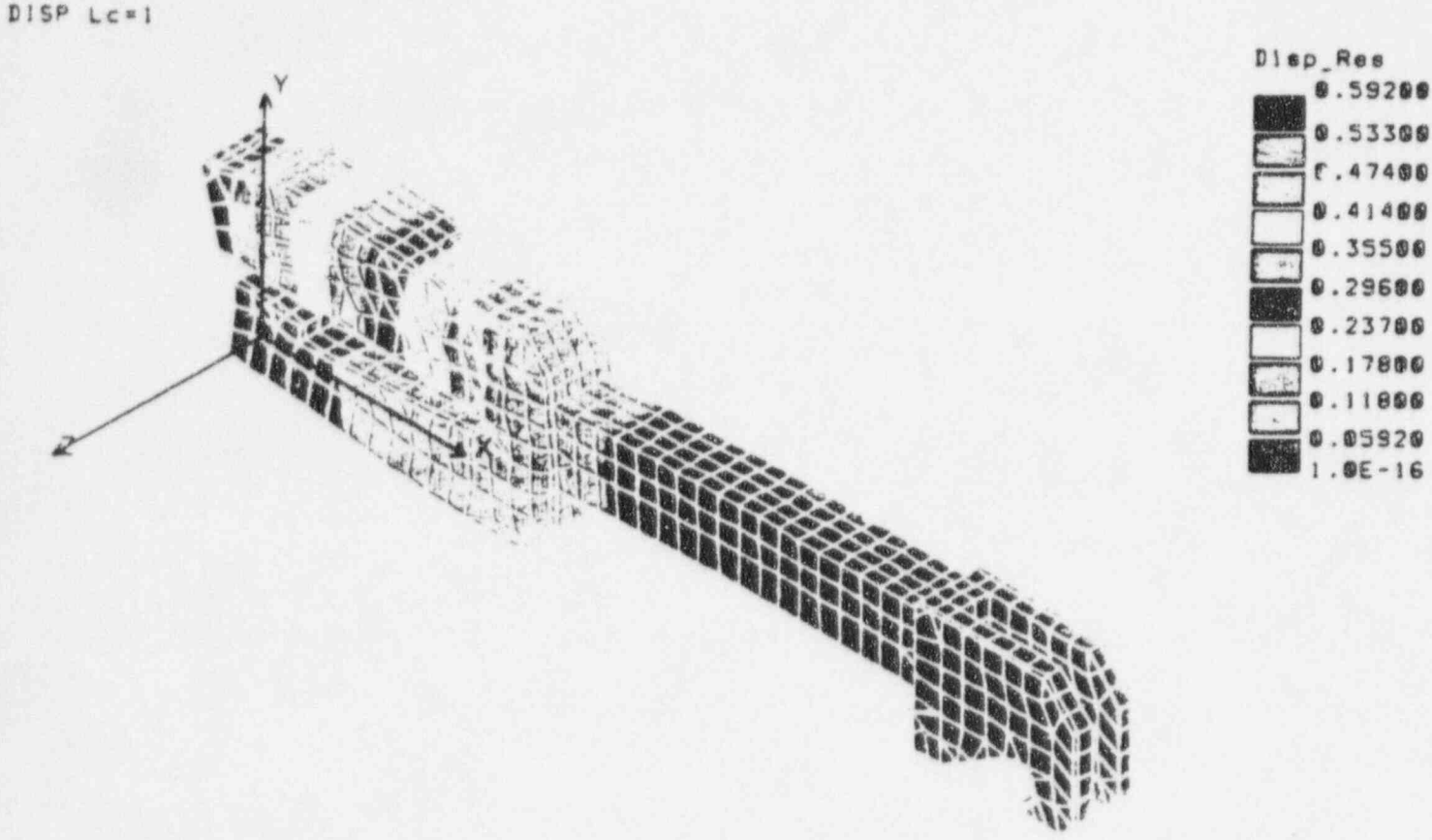

Figure 6.2-6 Lower Spring Faulted Condition, Deformation (Magnified)

6.3 Long Upper Support

The long upper support (Drawing 112D6669) is subjected to the following upper spring horizontal seismic load and the tie rod axial load [5,7].

Case	Seismic Load* (kips)	Tie Rod Load** (kips)
Normal / Upset	16.75	97.00
Emergency	33.50	169.50
Faulted	35.00	169.50
Thermal Upset	0.00	85.00

* The load shown is for one of the four upper supports (two long and two short),

** The load shown is for one of the two upper supports (two long).

The horizontal load produces low bearing and compressive stresses. The critical stress occurs in the vicinity of the lip at the shroud flange interface due to the tie rod axial load. Following are the resulting stress intensities and the comparison with allowables for the normal/upset, emergency, faulted, or thermal upset conditions.

Case	P_m (ksi)		S_{allow} (ksi)	
Normal / Upset	30.81	<	47.50	1.00 S_m
Emergency	54.97	<	71.25	1.50 S_m
Faulted	55.49	<	95.00	2.00 S_m

Case	P_m+P_b (ksi)		S_{allow} (ksi)	
Normal / Upset	47.11	<	71.25	1.50 S_m
Emergency	84.98	<	106.88	2.25 S_m
Faulted	85.92	<	142.50	3.00 S_m

Case	P_m+P_b+Q (ksi)		S_{allow} (ksi)	
Thermal Upset	33.64	<	142.50	3.00 S_m

Note that the maximum stress intensity during the thermal upset condition is below the material's proportional limit of 74 ksi, and the preload on the shroud will thus be maintained in such event.

The finite element (FE) model and the stress results of the long upper support are shown in Figures 6.3.1 and 6.3.2, respectively.

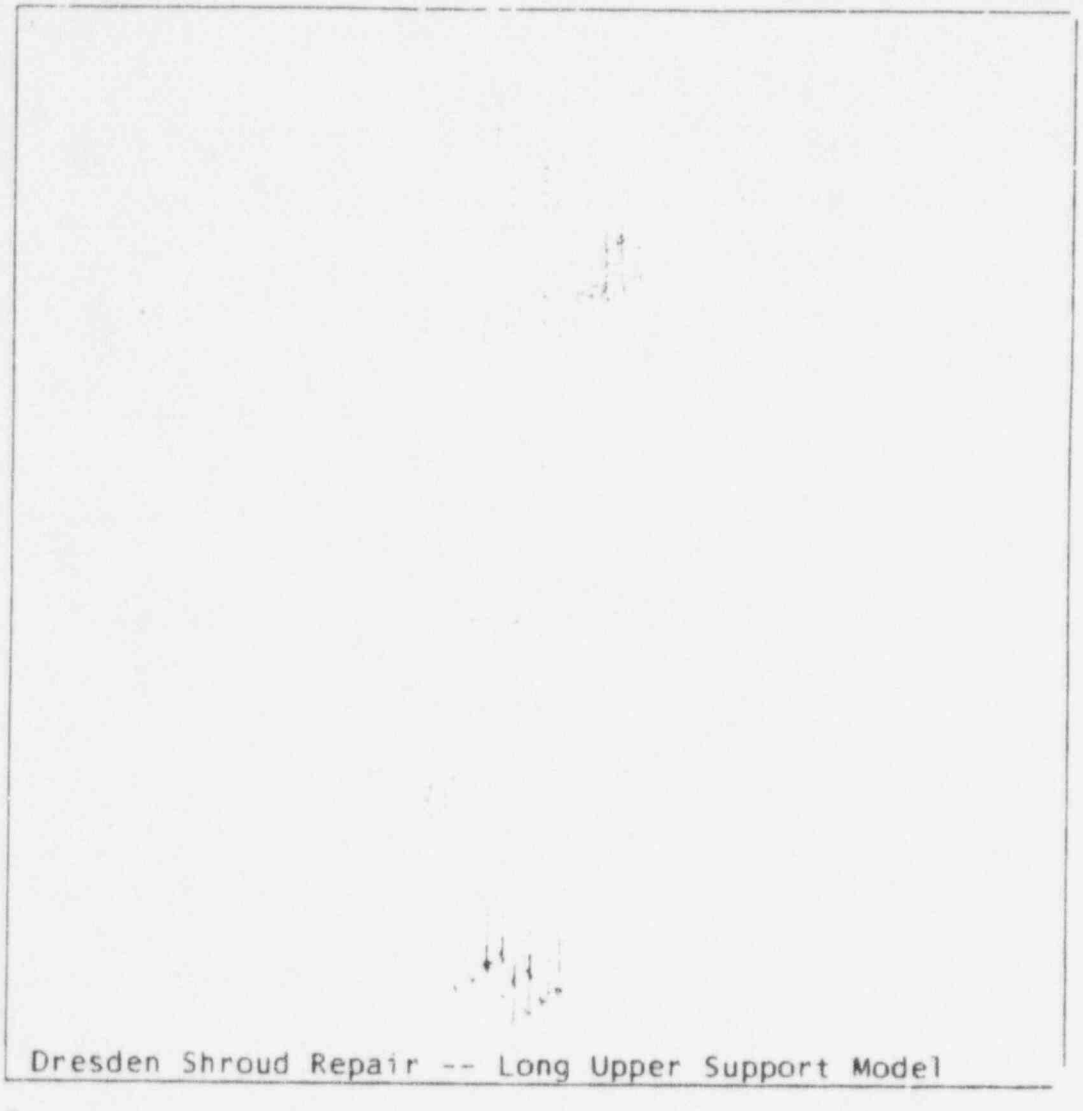

Figure 6.3.1 Long Upper Support FE Model and Boundary / Loading Conditions

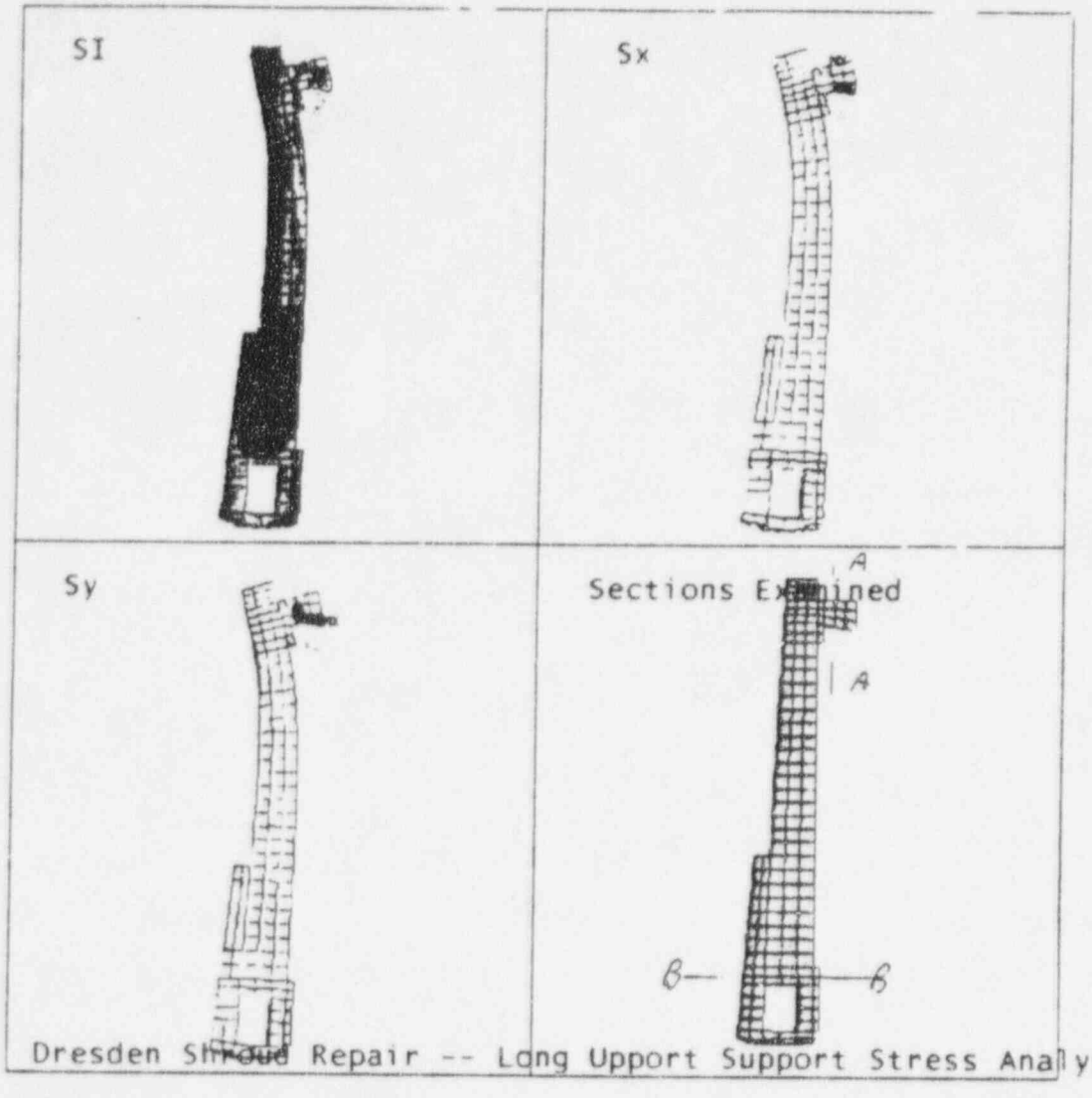

Figure 6.3.2 Long Upper Support FE Analysis Stress Plots

6.4 Bracket Yoke

The bracket yoke (Drawing 112D6675) is subjected to the following tie rod axial load [7].

Case	Tie Rod Load (kips)
Normal / Upset	194.00
Emergency	339.00
Faulted	339.00
Thermal Upset	170.00

The critical primary membrane stress occurs in the vicinity of the yoke support at the long upper support interface. Following are the resulting stress intensities and the comparison with allowables.

Case	P_m (ksi)		S_{allow} (ksi)	
Normal / Upset	15.32	<	47.50	1.00 S_m
Emergency	26.76	<	71.25	1.50 S_m
Faulted	26.76	<	95.00	2.00 S_m

The critical primary membrane plus primary bending stress occurs in the vicinity of the yoke at the tie rod interface. Following are the resulting stress intensities and comparison with allowables for the normal/upset, emergency, faulted or thermal upset conditions.

Case	P_m+P_b (ksi)		S_{allow} (ksi)	
Normal / Upset	31.35	<	71.25	1.50 S_m
Emergency	54.78	<	106.88	2.25 S_m
Faulted	54.78	<	142.50	3.00 S_m

Case	P_m+P_b+Q (ksi)		S_{allow} (ksi)	
Thermal Upset	27.47	<	142.50	3.00 S_m

Note that the maximum stress intensity during the thermal upset condition is below the material's proportional limit of 74 ksi, and the preload on the shroud will thus be maintained in such event.

The finite element model and the stress results of the bracket yoke are shown in Figures 6.4.1 and 6.4.2, respectively.

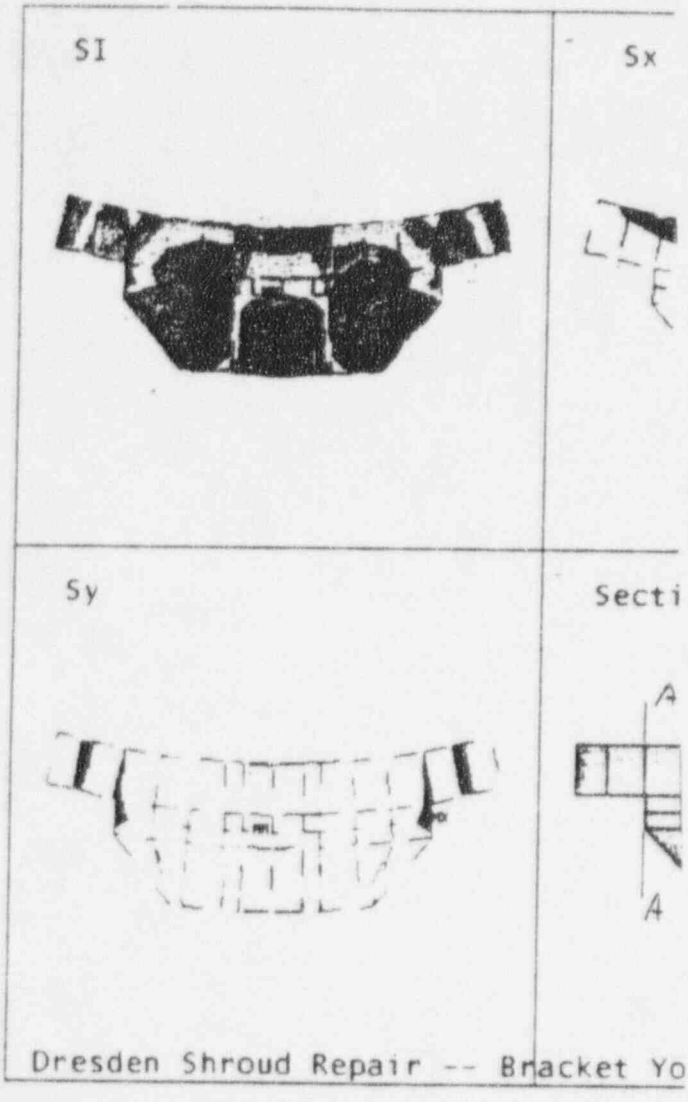

Figure 6.4.2 Bracket Yoke FE Analysi

GE Nuclear Energy

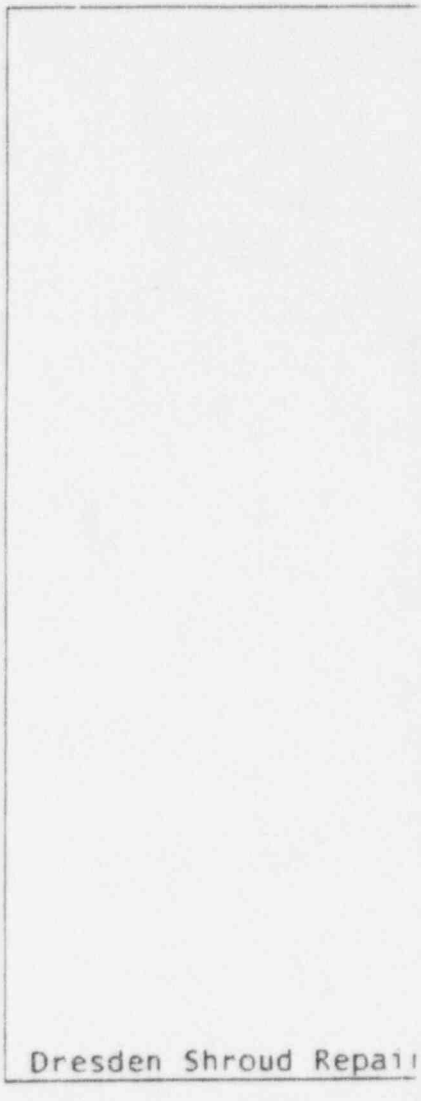

Figure 6.4.1 Bracket Yoke F

6.5 Middle Spring

The middle spring (Drawing 112D6681) is subjected to the following horizontal seismic loads [5]:

Case	F (kips)
Normal / Upset	12.00
Emergency	23.00
Faulted	24.00

The primary membrane plus primary bending stress intensity at the leaf spring region of the spring govern. The values and comparison with allowables follow.

Case	P_m (ksi)		S_{allow} (ksi)	
Normal / Upset	4.41	<	47.50	1.00 S_m
Emergency	8.45	<	71.25	1.50 S_m
Faulted	8.82	<	95.00	2.00 S_m

Case	P_m+P_b (ksi)		S_{allow} (ksi)	
Normal / Upset	37.46	<	71.25	1.50 S_m
Emergency	71.81	<	106.88	2.25 S_m
Faulted	74.93	<	142.50	3.00 S_m

The horizontal stiffness of the middle spring is 80 kips/inch based on finite element analysis. Accounting for the shroud local flexibility at the spring interface, the effective horizontal stiffness at the middle spring is 37 kips/inch. This is very close to the 35 kips/inch value used in the seismic analysis. The finite element model of this middle spring and its stress results are shown in Figures 6.5.1 and 6.5.2, respectively.

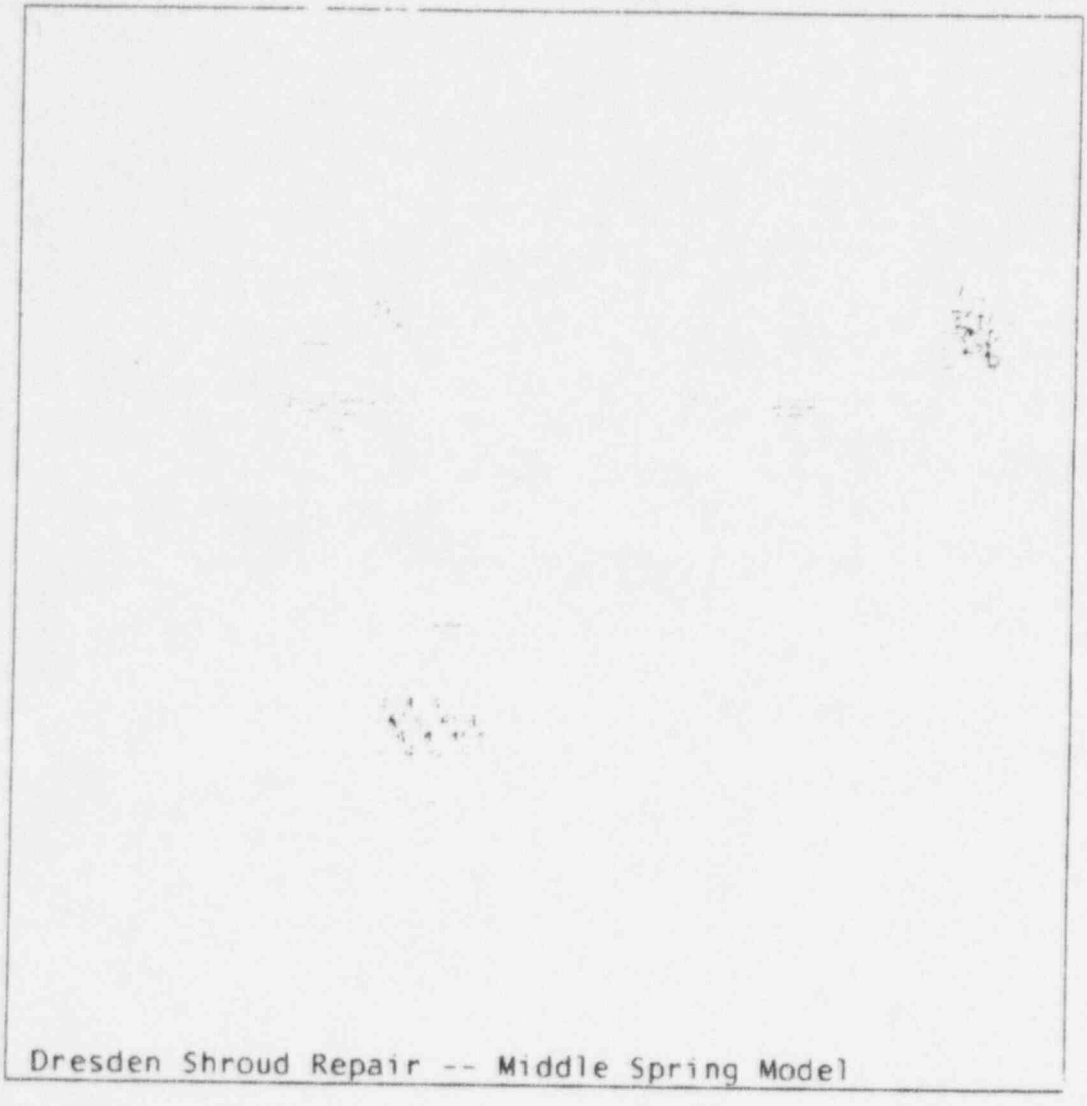

Figure 6.5.1 Middle Spring FE Model and Boundary / Loading Conditions

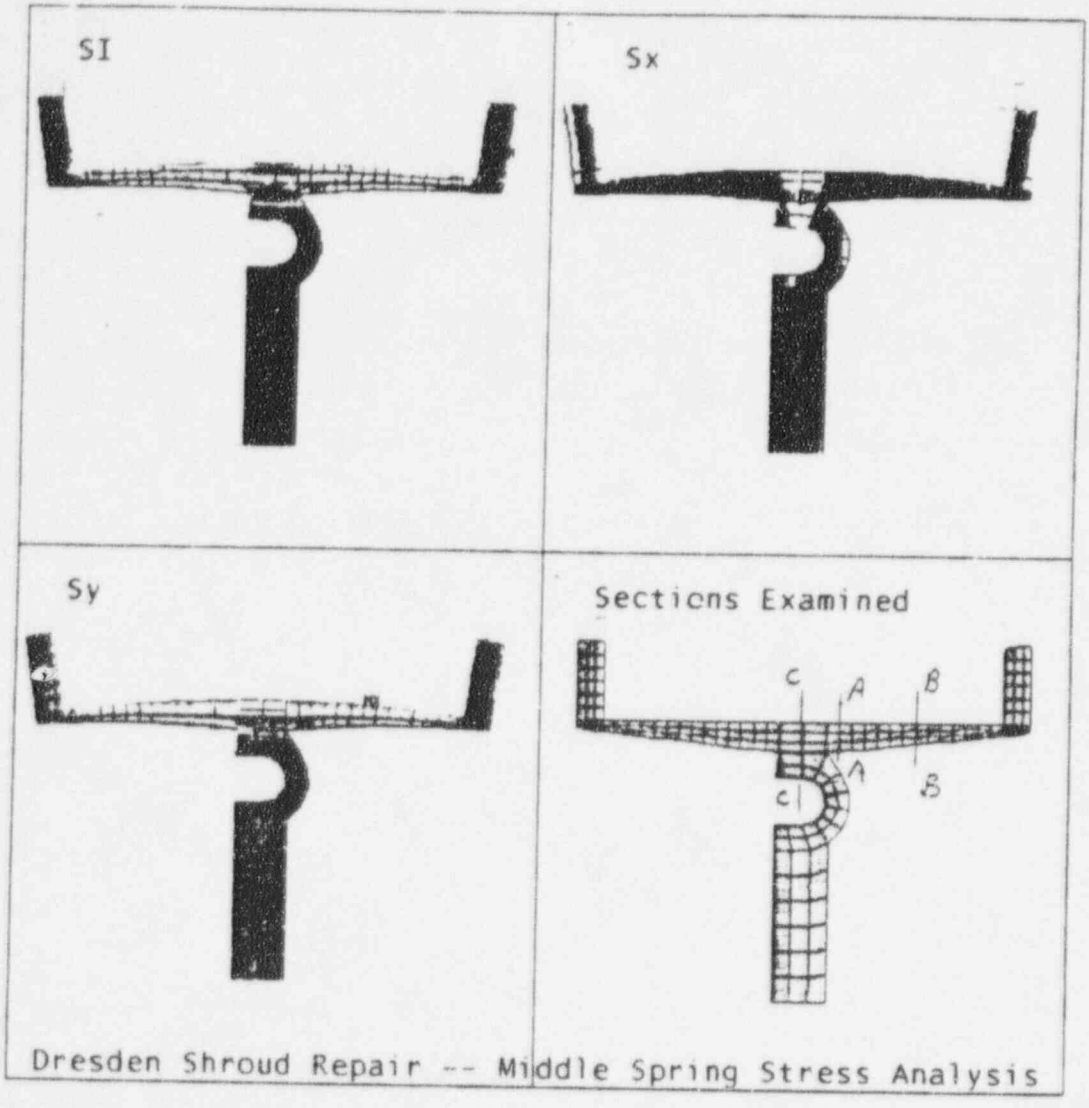

Figure 6.5.2 Middle Spring FE Analysis Stress Plots

6.6 Tie Rod

The tie rod (Drawing 112D6672) is subjected to the following middle spring horizontal seismic load and the tie rod axial load [5,7].

Case	Seismic Load (kips)	Tie Rod Load (kips)
Normal / Upset	12.00	194.00
Emergency	23.00	339.00
Faulted	24.00	339.00
Thermal Upset	0.00	170.00

The maximum rod primary membrane stress intensities during the normal/upset, emergency, or faulted conditions are as follows,

Case	P_m (ksi)		S_{allow} (ksi)	
Normal / Upset	20.17	<	29.58	1.0 S_m
Emergency	35.24	<	44.37	1.5 S_m
Faulted	35.24	<	59.16	2.0 S_m

And the corresponding rod critical primary membrane plus bending plus secondary stress intensity during a thermal upset event is as follows,

Case	$P_m + P_b + Q$ (ksi		S_{allow} (ksi)	
Thermal Upset	17.67	<	88.74	3.0 S_m

Note that the maximum stress intensity during the thermal upset condition is below the material's proportional limit of 31.44 ksi, and the preload on the shroud will thus be maintained in such event. The Tie Rod assembly stiffness is 650 kips/inch, which is very close to the value used in the seismic analysis (609 kips/inch).

Since the tie rod is subjected to a cross flow of coolant, its susceptibility to flow induced vibration was investigated. Natural vibration frequencies were derived using the finite element analysis (the model used is shown in Figure 6.6.1). The tie rod axial load of 138 kips under normal/upset condition was included in the model. The lowest natural frequency was found to be 35.5 Hz. To conservatively derive the flow vortex shedding frequency for comparison with the natural frequency, the bulk flow velocity of 4.9 feet/second near the tie rods adjacent to the jet pump inlet was assumed to be directed normal to the tie rod. The resulting vortex shedding frequency of 4.6 Hz is judged to be sufficiently lower than the lowest natural frequency such that no flow induced tie rod vibrations are expected. For the fatigue evaluation in the thermal upset event, the allowable number of fatigue cycles has been determined to be greater than 2,000 [Figure I-9.2.2 in Reference 3], which far exceeds the actual number of cycles anticipated. Therefore, the fatigue requirements are satisfied.

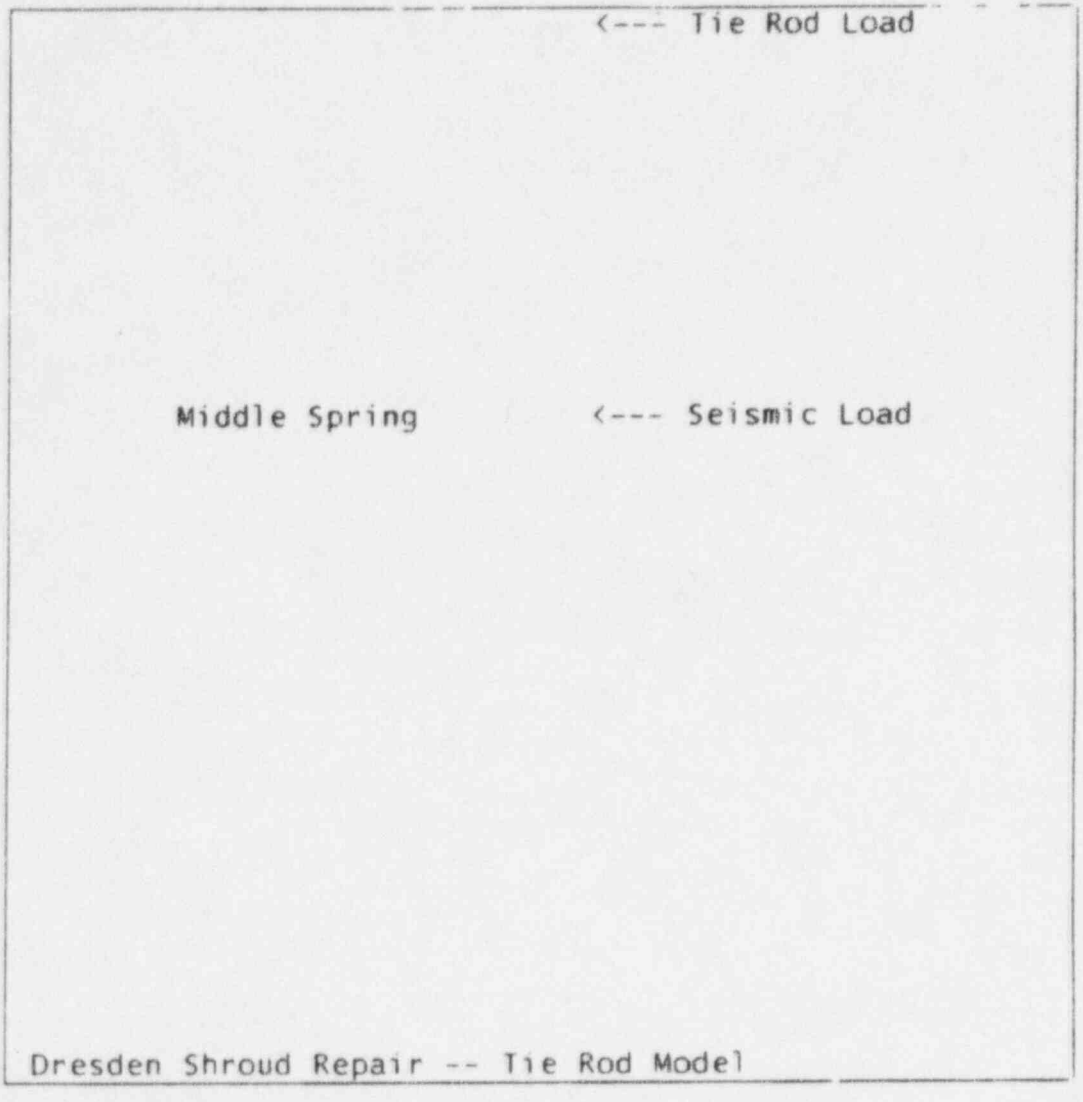

Figure 6.6.1 Tie Rod FE Model and Boundary / Loading Conditions

6.7 Lower Support and Toggle Assembly

The toggle bolt is the limiting component for this evaluation. The results for this X-750 material component are as follows:

Component	Limiting Load	Stress (ksi)		S_{allow} (ksi)
Horizontal Plate	P_m+P_b	67.54	<	106.88
Vertical Plate	P_m	43.30	<	71.25
Clevis Pin	P_m+P_b	67.38	<	106.88
(normal/upset)	Shear	12.65	<	36.92
(emergency)	Shear	22.10	<	48.00
(faulted)	Shear	22.10	<	48.00
Toggle Pin	P_m+P_b	70.39	<	106.88
(normal/upset)	Shear	20.14	<	36.92
(emergency)	Shear	35.19	<	53.44
(faulted)	Shear	35.19	<	71.25
Toggle Assembly	P_m	46.10	<	71.25
Toggle Assembly Fork	P_m+P_b	67.00	<	106.88
Toggle Bolt	P_m+P_b	104.63	<	106.88

The toggle bolt stress calculation is based on a very low preload of the bolts. If the bolt preload is increased suffciently the bolt stress will be reduced accordingly.

7.0 REFERENCES

1. ANSYS, General Purpose Finite Element Program, Version 4.4. Swanson Analysis Systems, Inc.

2. "Dresden Units 2 and 3, Shroud Stabilizer Hardware Design Specification", 25A5688, Rev.2.

3. ASME Boiler and Pressure Vessel Code, Section III, Appendices, 1989 Edition.

4. GENE Y1002A051, Rev.1.

5. "Dresden Units 2 and 3 Shroud Repair Seismic Analysis", GENE-771-84-1194, Rev.2.

6. "ComEd Technical Requirements Document for Dresden / Quad Cities Core Shroud Repair", NEC-12-4056.

7. " Back-up Calculations for Dresden Units 2 and 3 Pressure Vessel Stress Report", GENE-771-77-1194, Rev.2.

8. "Project Instruction Shroud Repair For H1 Through H7 Welds For Commonwealth Edison Dresden Units Nuclear Power Station", GENE-771-80-1194, Rev. 1.

9. "Dresden Units 2 and 3 UFSAR", Commonwealth Edison , Rev. 0.

10. COSMOSM, General Purpose Finite Element Program, Version 1.7.1, Structural & Analysis Corporation.

11. "Section E.2 of Design Record File (DRF) for the Dresden Shroud Repair Program", DRF B13-01749.

12. "Dresden Units 2 and 3, RPV Code Design Specification", 25A5689, Rev.2.

Enclosure 6

GENE 771-81-1194, Revision 1

Commonwealth Edison Company
Dresden Nuclear Power Plant Units 2 & 3
Shroud and Shroud Repair Hardware Analysis, Volume II, Shroud

Commonwealth Edison Co.
Dresden Nuclear Power Station Units 2 and 3
Shroud and Shroud Repair Hardware Analysis for the Repair of Welds H1 through H7

Volume II: Shroud

May 1995

Prepared by: F. Shahrivar — 5-12-95 Date

Verified by: M. Patel, S. Hlavaty, Y. Wu — 5-12-95 Date

Approved by: M.D. Potter for — 5/12/95 Date
R.P. Svarney, GE Project Manager
Dresden Shroud Repair Project

GE Nuclear Energy

San Jose, California

ABSTRACT

This document provides the results of the stress analysis of the Dresden Shroud and Shroud Repair Hardware, demonstrating that structural integrity limits are maintained under the loading and stress limits specified in Design Specification 25A5668.

EXECUTIVE SUMMARY

This report provides the results of the stress analysis of the Dresden shroud [Vol. II, i.e., this volume, also in Reference 10] and shroud repair hardware [Vol. I] when subjected to all applied loading including seismic, pressure, deadweight, and thermal effects.

The shroud restraint hardware consists of four identical sets of tie rod and spring assemblies. The four sets are spaced 90° apart, beginning at 20° from vessel zero. Each set consists of the following major elements:

1. An Upper Spring, located in the reactor pressure vessel (RPV)/shroud annulus at the top guide elevation. This spring provides lateral seismic support to the shroud at the top guide elevation and transmits seismic loads from the nuclear core directly to the RPV.

2. An Upper Support Assembly, located in the annulus from the top guide elevation to the top of the shroud. This assembly provides a connection for the tie rod to the shroud top.

3. A Middle Spring, located in the annulus at the elevation of the jet pump support brackets. This spring provides lateral seismic support to the shroud, keeps the shroud from coming in contact with the jet pump support brackets during a seismic event, and restrains the tie rod movement for proper tie rod vibration characteristics.

4. A Lower Spring, located in the annulus at the core plate and shroud support region. This spring provides lateral seismic support to the shroud, transmitting core seismic loads to the RPV. In addition, this spring provides a connection for the tie rod to the shroud support plate.

5. The Tie Rod, which connects to the upper end of the top of the shroud and to the lower end of the lower spring. This component develops a thermal preload due to normal operating temperature, which in turn provides vertical clamping forces to the shroud.

The upper, middle, and lower spring designs have been optimized to minimize the seismic interaction between the shroud and RPV while still meeting stress limits.

The stress analysis of the overall core shroud was performed with the ANSYS code [Reference 1]. A three-dimensional finite element model was constructed which included the shroud from the upper flange at the shroud head joint down to the connections at the RPV. Because of the symmetrical behavior of the shroud under the applied loads, a 180° circumferential segment was modeled.

The stress analysis of the major shroud repair hardware components was performed with the ANSYS code [Reference 1]. For the smaller components, hand calculations were performed.

The load combinations and structural acceptance criteria are contained in the Design Specification [Reference 2]. The results of the stress analysis demonstrate that the shroud and shroud repair hardware meet the requirements of that specification.

The analysis results are reported in Volume 1 of this report for the repair hardware and in Volume 2 (this Volume) for the shroud.

IMPORTANT NOTICE REGARDING THE CONTENTS OF THIS REPORT

The only undertaking of the General Electric Nuclear Energy (GENE) respecting information in this document are contained in the contract between Commonwealth Edison (ComEd) and GENE, and nothing contained in this document shall be construed as changing this contract. The use of this information by anyone other than ComEd, or for any purpose other than that for which it is intended, is not authorized; and with respect to any unauthorized use, GENE makes no representation or warranty and assumes no liability as to the completeness, accuracy, or usefulness of the information contained in this document.

Table of Contents

List of Figures

1.0 INTRODUCTION

Inter granular stress corrosion cracking (IGSCC) has been found in the core shroud welded joints of several Boiling Water Reactors. Similar cracking may also exist in the welded joints of the Dresden Core Shroud. GENE has designed a shroud repair system that reinforces the shroud in the event that any or all of the seven shroud horizontal weld joints are cracked. The component referred herein (and in Reference 10) as "shroud" is the internal shroud portion starting with the head flange, at its uppermost part, down to the level positioned at the top of the shroud support legs (these legs are addressed in References 4 and 7). The stress analysis discussed in this report demonstrates that the shroud and the shroud repair system (refer to Vol. I of this report) structural integrity is maintained if any or all of these seven welded joints (H1 through H7) are cracked completely through their thickness and around their entire 360° circumference. The structural integrity of the shroud and shroud repair system is also demonstrated in the event that the shroud is uncracked and the repair system is installed.

2.0 SHROUD REPAIR HARDWARE DESIGN FEATURES

The shroud repair system consists of four identical sets of tie rod and spring assemblies. The four sets are spaced at 90° intervals beginning at 20° from vessel zero. A layout of one of the tie rod and spring sets is shown in Figure 2.1.

The tie rods are thermally preloaded to provide vertical compressive clamping forces on the shroud. The magnitude of the tie rod thermal preload is greater than the net uplift forces on the shroud due to normal operating pressures, so that no vertical separation of shroud sections would occur if the welded joints are postulated to be completely cracked. This is not the case for postulated LOCA main steam line break uplift pressures, which are sufficient to overcome the tie rod preload and momentarily separate shroud sections.

The upper, middle, and lower springs provide a lateral seismic load path from the top guide and core plate to the RPV. The magnitude of the seismic loads in these springs is a function of their stiffness. The stiffness has been optimized to minimize the seismic loads while still meeting the stress and displacements limits. The U-shaped upper springs consists of tapered legs that flex towards each other under lateral seismic loads. The taper in these legs has been optimized to produce constant stress along their length while providing the required stiffness. For the middle spring, the flexibility of the taper legs provides the needed lateral stiffness to keep the middle section of the shroud from coming in contact with the jet pump support brackets during a seismic event. This keeps the shroud from moving closer than 1/2-inch to the jet pump support bracket. The rigid middle section of the middle spring also provides an intermediate lateral support to the tie rod. The natural vibration frequency of the tie rod with this intermediate support is then well removed from the flow-induced forcing frequency (flow induced vibration is discussed in detail in Section 7 of Volume I). For the lower spring, the flexibility of the Y-shaped feature at the top provides the lateral stiffness property, whereas the bending flexibility of the straight middle section provides the axial stiffness property, which in combination with the stiffness of the tie rod and upper axial component determines the tie rod thermal preload.

The shroud geometry and location and designation of the seven shroud horizontal weld joints are shown in Figure 2.2.

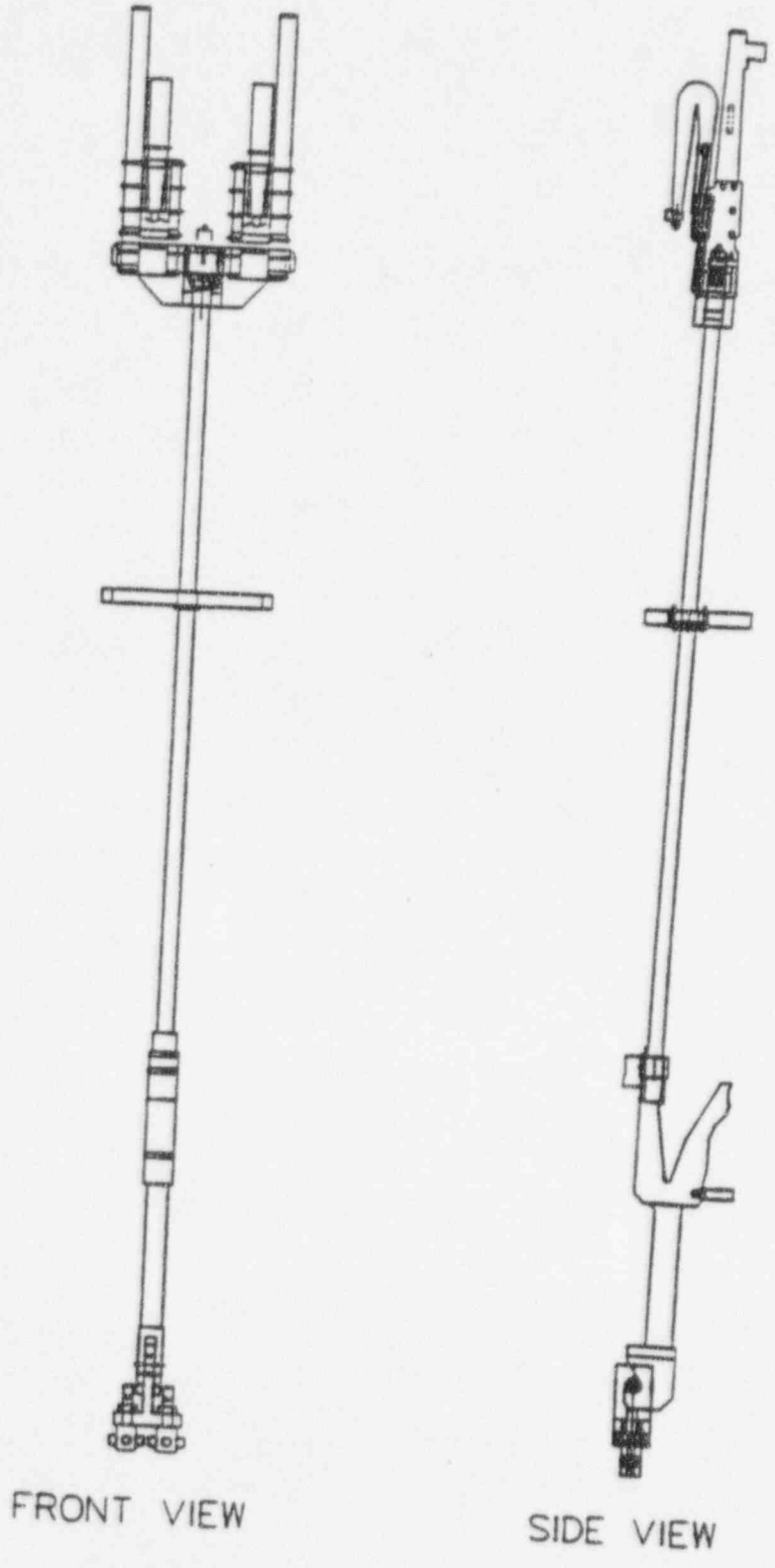

Figure 2.1 Shroud Repair Hardware Layout

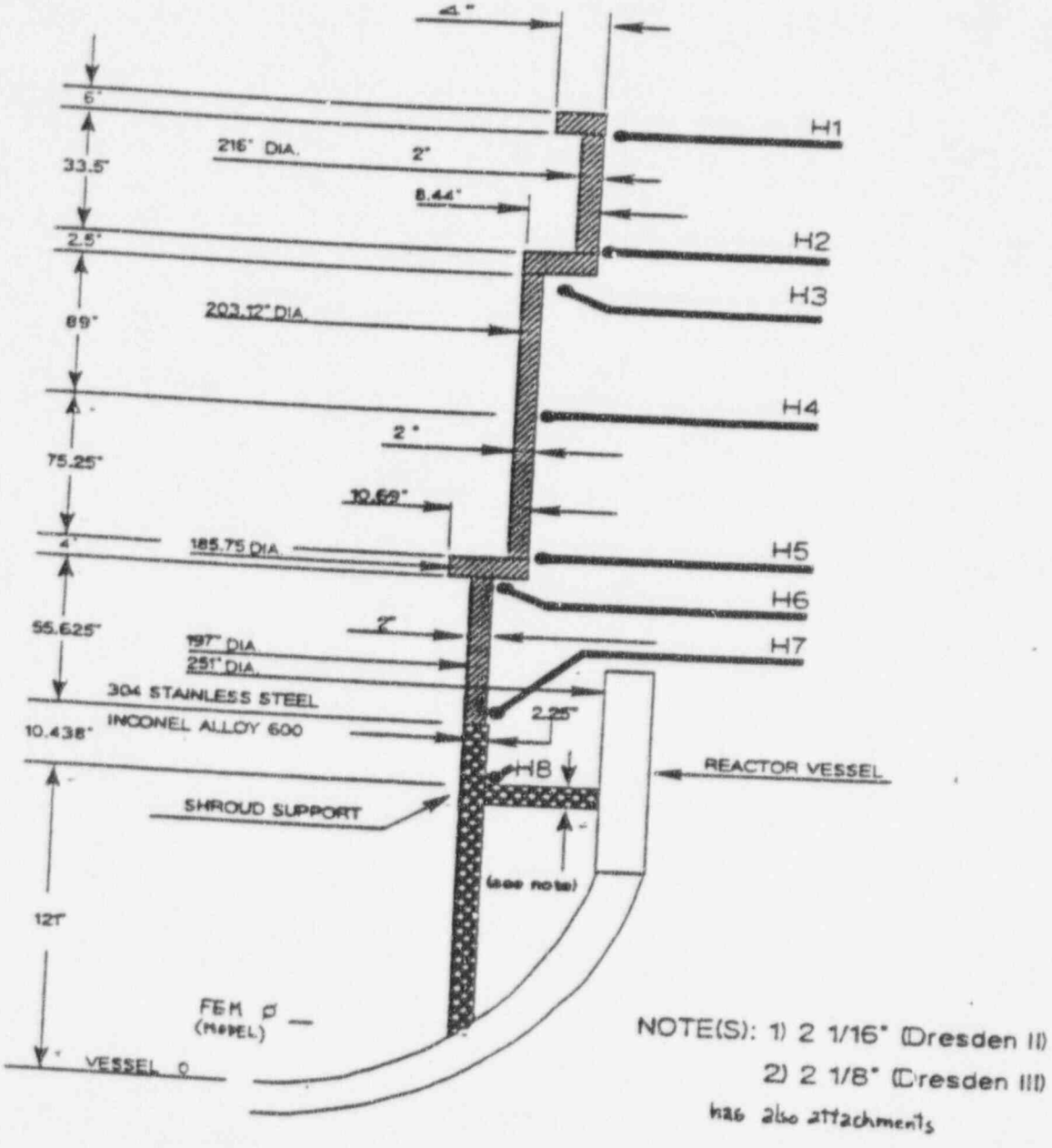

Figure 2.2 Shroud Horizontal Weld Designations

3.0 MATERIAL PROPERTIES

The following material properties for the primary load bearing restraint components are taken from Appendix I of the ASME B&PV Code [Reference 3] and GENE Testing Report [Reference 4]. A 550° F temperature applies to the Normal and Upset condition, as well as the Faulted and Emergency conditions.

3.1 **Shroud** (Drawing 718E861)

SS-304	at 550° F (oper.)	
Young's Modulus	25.5 E6 psi	Table I-6 [Reference 3]
Thermal Expansion Coefficient	9.46 E-6 in/in/°F	Table I-5 [Reference 3]
S_m	16950 psi	Table I-1.2 [Reference 3]

3.2 **Tie Rod** (Drawing 112D6672)

XM-19	at 550° F (oper.)	
Young's Modulus	25.6 E6 psi	Table I-6 [Reference 3]
Thermal Expansion Coefficient	8.98 E-6 in/in/°F	Table I-5 [Reference 3]
S_m	29450 psi	Table I-1.2 [Reference 3]

3.3 **Spring and Upper Assemblies** (Upper Spring Drawing 112D6670; Long Upper Support Drawing 112D6669, Bracket Drawing 112D6675; Middle Spring Drawing 112D6681; and Lower Spring Drawing 112D6671)

X-750	at 550° F (oper.)	
Young's Modulus	28.4 E6 psi	[Reference 4]
Thermal Expansion Coefficient	7.5 E-6 in/in/ °F	[Reference 4]
S_m	47500 psi	[Reference 4]

3.4 **Inconel Alloy 600** (Drawings 105E1415A through D)

Inconel 600 (N06600)	at 550° F (oper.)	
Young's Modulus	28.8 E6 psi	[Reference 4]
Thermal Expansion Coefficient	7.77 E-6 in/in/ °F	[Reference 4]
S_m	23300 psi	[Reference 4]

4.0 LOADS AND LOAD COMBINATIONS

The Design Specification [Reference 2] specifies that the shroud and shroud repair hardware shall be analyzed for the following load combinations:

Normal / Upset	ΔP_N + DW + OBE
Emergency 1	ΔP_N + DW + SSE
Emergency 2	$\Delta P_{MS\text{-}LOCA}$ + DW
Emergency 3	$\Delta P_{RC\text{-}LOCA}$ + DW
Faulted 1	$\Delta P_{MS\text{-}LOCA}$ + DW + SSE
Faulted 2	$\Delta P_{RC\text{-}LOCA}$ + DW + SSE

where:
- ΔP_N = Normal Pressure Difference
- DW = Dead Weight Loads
- OBE = Operating Basis Earthquake
- SSE = Safe Shut-down (Design Basis) Earthquake (DBE)
- $\Delta P_{MS\text{-}LOCA}$ = Main Steam Line LOCA
- $\Delta P_{RC\text{-}LOCA}$ = Recirculation Line LOCA = $\Delta P_{RRLB\text{-}LOCA}$
- LOCA = Loss of Coolant Accident

The OBE and SSE loads are reported in Reference 5. Since the configuration of the seismic model depends on the assumed behavior at weld joints postulated to be cracked, and the resulting seismic loads depend on this assumed behavior, two sets of SSE seismic loads were established. The first set corresponds to the configuration for normal pressure differences and was used in the Emergency 1 load combination. The second set of seismic loads corresponds to the configuration for Main Steam Line LOCA pressure differences and was used in the Faulted 1 load combination. The configuration of the seismic model for the recirculation line outlet LOCA corresponds to that for normal pressure differences, and hence the seismic loads to be combined in the Faulted 2 load combination for the recirculation line outlet LOCA are from the first set of seismic loads.

After reviewing the FSAR, it was determined that the shroud loads due to a feedwater line break are bounded by the main steam line break loading and the recirculation line break loading.

The appropriate deadweight loads were used in this stress analysis. The effects of the vertical seismic accelerations on the deadweight were also included.

The pressure difference loads are taken from the Design Specification [Reference 2].

5.0 STRUCTURAL ACCEPTANCE CRITERIA

The Design Specification specifies the following stress intensity limits in the Shroud.

	Resulting Stress			S_{allow}
Upset	Primary Membrane	P_m	<	1.00 x S_m
	Primary Membrane + Primary Bending	$P_m + P_b$	<	1.50 x S_m
	Local Primary Membrane + Primary Bending	$P_l + P_b$[1]	<	1.50 x S_m
	Primary + Secondary	P + Q	<	3.00 x S_m
Emergency	Primary Membrane	P_m	<	1.50 x S_m
	Primary Membrane + Primary Bending	$P_m + P_b$	<	2.25 x S_m
	Local Primary Membrane + Primary Bending	$P_l + P_b$[1]	<	2.25 x S_m
Faulted	Primary Membrane	P_m	<	2.00 x S_m
	Primary Membrane + Primary Bending	$P_m + P_b$	<	3.00 x S_m
	Local Primary Membrane + Primary Bending	$P_l + P_b$[1]	<	3.00 x S_m

[1] This is not an ASME subsection NG requirement, rather a GE requirement for the regions in close proximity to the point of application of concentrated loads, e.g., tie rod loads.

The maximum lateral deflection, relative to the core plate, of any point on the shroud adjacent to either the H2 or H3 weld during seismic events is limited to the following values [Reference 6]:

Upset	δ	<	0.90 inches
Emergency	δ	<	1.90 inches
Faulted	δ	<	1.90 inches

The work reported in Reference 5 addresses the conformance with these deflection limits.

6.0 SHROUD ANALYSIS

6.1 Model Description

The finite element model of the shroud is shown in Figure 6.1. This three-dimensional model was developed and analyzed using the ANSYS code [Reference 1]. The model uses shell elements to represent the shell portions of the shroud, and solid elements to represent the thicker segments, namely, the flanges or heavy rings at the shroud head, the top guide, and the core plate. Since the structure and deformations have planar symmetry, only a 180° circumferential section of the shroud needs to be represented. Appropriate symmetry boundary conditions are applied along all of the edges of the model at the symmetry plane, i.e., y-translation, x- and z-rotation constrained. The shroud support plate and the shroud support legs are included in the model with boundary constraints applied at the vessel side of the support plate (x-, z-translation, and x-, y-, z-rotations constrained) and the lower end of the support legs (fixed). All seven welds H1 through H7 are assumed cracked for bounding the stress analysis results as follows: The boundary nodes of the shroud segments coinciding on a crack are coupled only in their translational degrees of freedom to model the crack. This enforces zero shell bending stresses across the crack faces and prevents any transfer of shell bending moment across the seven welds H1 through H7.

Five separate load sets were applied corresponding to the following bounding load cases: a) Normal and Upset seismic, b) Emergency 1, c) Emergency 2, d) Faulted 1, and e) Upset Thermal. This last set, namely (e), was done to investigate for the cracked shroud the effect of the 10 upset thermal transients expected during the life of the plant.

6.2 Applied Loads

Vertical loads covering the vertical seismic, deadweight, buoyancy, and those due to pressure differences are applied to the model at their point(s) of action and distributed around the model as appropriate. The shroud head pressure uplift force, the shroud head forces due to deadweight and vertical seismic acceleration are applied vertically at the shroud top uniformly along the circumferential direction as shown in Figure 6.2. The net tie rod forces are applied vertically at the top of the shroud. Net tie rod forces are obtained by adding the appropriate components, e.g., seismic, initial mechanical preload, and the effect on the tie rods of the net shroud uplift force. In accordance with the ASME Code [Subsection NG, Reference 3] the thermal component of load causing secondary stresses are not considered in the evaluation of the primary stress intensities.

Radial pressures are applied to the shroud on both the interior and exterior of the shroud throughout the height. These pressures represent the reactor internal pressure and its change as one moves radially from inside the shroud shell to its outside.

Since the top part of the shroud is not included in the model, the internal moment and shear that it exerts on the modelled portion of the shroud are applied to the model as circumferentially varying vertical and horizontal loads along the top flange as shown in Figure 6.3.

The lateral loads covering seismic (see Figure 6.3, also Reference 10), spring reactions, and those due to pressure differences during a Recirculation Line Outlet LOCA are applied to the model at their point(s) of action and distributed around the model as appropriate as shown in Figure 6.4. In each case, the shear and moment diagrams, respectively, effected by the applied lateral loads, envelop the shroud shear and moment diagrams specified for the case considered.

For Recirculation Line Outlet LOCA a spatial and time varying horizontal differential pressure is developed on the shroud with a resultant lateral force component. The initial acoustic phase of this LOCA transient is very abrupt relative to the shroud vibration frequency with a very small dynamic amplification factor, implying only a small equivalent static force. The remainder of the pressure transient extends over a relatively large time span and as such can be considered as a static load. The resulting lateral forces of the two sets, namely, the acoustic and the transient sets were compared and the transient forces (blowdown loads) were found to be the bounding force set. This bounding horizontal LOCA force set due to the transient pressures is applied to the model as static loads in the manner shown in Figure 6.4.

Pressure differentials including loads of the Recirculation Line Outlet LOCA are contained in References 2 and 9. Seismic loads can be found from the Dresden Shroud Repair Seismic Report [Reference 5]. The bounding seismic loads on the restraint components are also included in the Design Specification.

6.3 Results and Comparison to Allowables

The shroud stress intensity results and their comparison to allowables for the required load combinations are reported in the following paragraphs. As will be noted, the Pm+Pb and Pl+Pb stress intensities are generally less than the allowable value on the Pm stress intensity alone. The stress intensities and comparisons to the allowables are:

Normal + Upset (ΔP_N + DW + OBE)

The maximum Pm+Pb stress intensity above the core plate level, occurs in the shroud shell at the middle spring location:

Pm + Pb = 8280 psi < 1.0 Sm of 16950 psi (limit for Pm alone),
allowable is 1.5 Sm of 25400 psi

The next highest stress intensity in this zone is only Pl+Pb= 3870 psi and is located at the upper shroud shell immediately under the head flange where the tie rod with the highest load engages. In this case, in the lower areas, a maximum stress intensity can be found at the shroud juncture with the shroud support leg for an uncracked shroud in an OBE event with

Pl + Pb = 12000 psi < 1.0 Sm of 16950 psi (limit for Pm alone),
allowable is 1.5 Sm of 25400 psi

Upset Thermal

A shroud model coupled with the tie rods (rather than applying external tie rod loads, strut elements with the properties of the tie rod assemblies were added to the model) was analyzed to determine the highest stresses in the shroud in an Upset Thermal event. The temperature distribution for this event was applied along with the Normal pressure (conservative simplification) and weight loads. In addition to stress results which help pinpoint the highest stress location in the shroud for fatigue usage evaluation, this analysis produces resultant tie rod forces for the condition analyzed.

Shroud leg contraction (relative to the RPV) effects are not included in this analysis to produce higher tie rod loads, and therefore higher stresses.

In this model, the H2, H3, H4, H5, and H6 welds are assumed cracked. The results show that the stress for this model and loading are highest in the top guide flange (refer to the end of this subsection). The discussion that follows is in relation to this stress. The pivot or contact location between flanges of the top guide and core plate and their adjoining cylindrical shells is located one inch from the centerline of the shells; i.e., where it would be if the finite (1 in.) size of the fillet weld was ignored. Although this pivot location is at the same radial position as in the case in which cracking is in the shroud shell at the top of the fillet welds, the results of the case considered are more conservative than this latter cracking scenario. This is because the cross section of the monolithic segment bounded by the cracks and comprised mainly of the flange (includes in the latter case, the welds as well as possibly a small shell segment) is

larger and stiffer in the latter case and leads to lower stresses. Even if the cracking is such that the fillet weld separates from the flange but remains attached to the cylindrical shell, the pivot locations will be at the toe of the fillet welds with the radial offset of the two resulting pivot locations (one above and one below the flange) being smaller than the case analyzed. A smaller radial offset renders a higher flange stiffness and lower stresses.

The maximum stress intensity (which is not limited from a structural strength standpoint, because it is a secondary stress) in the model from this analysis occurs at the top guide flange under the tie rods. This stress intensity is

P + Q = 14910 psi < 3 Sm of 50800 psi

The yield stress is 20300 psi at 433 degrees F implying no yielding, and therefore no permanent deformation of the shroud for this event. Yielding would have adverse implications relative to the opening of a gap at a cracked H6 weld during normal operation.

Emergency 1 (ΔP_N + DW + SSE)

The maximum Pm+Pb stress intensity above the core plate level, occurs in the shroud shell at the middle spring location:

Pm + Pb = 15930 psi < 1.5 Sm of 25400 psi (limit for Pm alone),
allowable is (2.25 Sm) 38100 psi.

The next highest stress intensity in this zone is only Pl+Pb= 7330 psi and is located at the upper shroud shell immediately under the head flange where the tie rod with the highest load engages. In this case, the other high stress areas have: Pm+Pb= 10410 psi stress intensity for the zone between the core plate and the shroud support plate levels; and below this zone, a maximum stress intensity can be found at the shroud juncture with the shroud support leg for an uncracked shroud in an SSE event with

Pl + Pb = 22300 psi < 1.5 Sm of 35000 psi, limit for Pm alone,
< Allowable is (2.25 Sm) 52400 psi

Emergency 2 and 3 ($\Delta P_{MS\text{-}LOCA}$ + DW) & ($\Delta P_{RC\text{-}LOCA}$ + DW)

The governing loading condition is that of the MS-LOCA case. For conservatism, the transient lateral loads of the RRLB_LOCA have been included with the MS-LOCA loads in the analysis.

In this case, the shroud model is severed from its lower portion at weld H6, where the high pressure induced loads at the core plate level are expected to lift it. The lower edge of the element nodes coinciding with the H6 weld are unconstrained. The lateral loads are reacted in this case by the upper, middle, and lower springs which have been introduced as springs that form the lateral restraint system.

The maximum Pm+Pb stress intensity above the core plate level, occurs in the shroud shell at the middle spring location:

Pm + Pb = 12700 psi < 1.5 Sm of 25400 psi limit for Pm alone,
< Allowable is (2.25 Sm) 38100 psi

In this case, the next highest stress area of concern has only a Pm+Pb= 3400 psi stress intensity and is located in the shroud cylinder near and above the point of application of the lower spring load.

Faulted 1 and 2 ($\Delta P_{MS\text{-}LOCA}$ + DW + SSE) & ($\Delta P_{RRLB\text{-}LOCA}$ + DW + SSE)

The governing loading of the Faulted condition is that of the MS-LOCA case. For conservatism, the transient lateral loads of the RLLB-LOCA have been included with the MS-LOCA loads in the analysis. Both cases were analyzed and results confirmed this, except at the middle spring which was slightly higher for Faulted 2. Therefore the results reported here are from Faulted 1 except for the middle spring contact point. The maximum Pm+Pb stress intensity above the core plate level, occurs in the shroud shell at the middle spring location:

Pm + Pb = 22590 psi, for Faulted 2
Pm + Pb = 22420 psi , for Faulted 1
both < 2 Sm of 33870 psi limit for Pm alone,
< Allowable is (3 Sm) 50800 psi.

In this zone and for this loading case, the next highest stress area of concern has a PI+Pb= 8520 psi stress intensity and is located at the shroud upper shell region under the location of the highest tie rod load. The other high stress areas have: Pm+Pb= 12900 psi stress intensity for the zone between the core plate and the shroud support plate levels; and below this zone, a maximum stress intensity can be found at the shroud juncture with the highest loaded shroud support leg for an uncracked shroud in an SSE event with

PI + Pb = 27000 psi < 3 Sm of 69900 psi (limit for Pm+Pb)

Detailed Analysis of the Shroud Support Plate: (all Cases)

To investigate the plate stresses in the shroud support plate in the vicinity of the tie rod system attachment due to the tie rod axial loads, separate ANSYS finite element analyses were completed. A description of the models and additional information can be found in Reference [10]. The stress in the plate due to the tie rod load is very localized and highest at the RPV-support plate juncture since the heavy RPV is close by. The resulting stress intensities (caused by tie rod force, pressure, and dead weight) and their comparisons to allowables follow. These results cover the two scenarios of the H8 horizontal weld locally cracked as well as uncracked. Stresses for fatigue evaluation are covered in the overall RPV stress report since the highest stress falls at the RPV-support plate juncture which is addressed in Reference 7.

Normal + Upset: (ΔP_N + DW + OBE)

	H8 cracked	H8 uncracked	
Pl =	7300 psi	6600 psi	< Sm of 23300 psi
Pm + Pb =	24300 psi	19300 psi	< 1.5 Sm of 34950 psi

Upset Thermal:

Contraction of the legs (relative to the RPV) was evaluated as causing a reduction in the tie rod load magnitude and the stress and was ignored. The highest stress occurs at the RPV-support plate juncture, and determines the fatigue usage for the shroud. This stress and the fatigue usage calculation is presented in Reference 7.

Emergency 1: (ΔP_N + DW + SSE)

	H8 cracked	H8 uncracked	
Pl =	14300 psi	13000 psi	< 1.5 Sm of 34950 psi
Pm + Pb =	47000 psi	37600 psi	< 2.25 Sm of 52425 psi

Emergency 2: ($\Delta P_{MS\text{-}LOCA}$ + DW)

	H8 cracked	H8 uncracked	
Pl =	5100 psi	4600 psi	< 1.5 Sm of 34950 psi
Pm + Pb =	17400 psi	13600 psi	< 2.25 Sm of 52425 psi

Emergency 3: ($\Delta P_{RC\text{-}LOCA}$ + DW)

Stresses are less than the Emergency 2 combination.

Faulted 1 & 2: ($\Delta P_{MS\text{-}LOCA}$ + DW + SSE)

	H8 cracked	H8 uncracked	
Pl =	14400 psi	13000 psi	< 2 Sm of 46600 psi
Pm + Pb =	47400 psi	37800 psi	< 3 Sm of 69900 psi

6.4 Gap at a Cracked H6 Weld

One of the concerns during normal operation is the possibility of flow out of the shroud interior through a gap that develops at a cracked H6 weld. A shroud model (see Figure 6.1) coupled with the tie rods was developed and analyzed to determine whether a gap would open at the cracked H6 weld during normal operation. In this model, the H2, H3, H4, H5, and H6 welds are assumed cracked. The model is severed at weld H6 (the edge nodes, positioned on this weld, of element rows falling above and below this weld are fully uncoupled from each other) to investigate whether a gap would open at a fully-cracked H6 weld. This model is also severed at weld H8 (the edge nodes, positioned on this weld, of the baffle plate elements are fully uncoupled) for conservatism.

The pivot or contact location between flanges of the top guide and core plate and their adjoining cylindrical shells is located at the intersection of the flange surface and shell centerline; i.e., where it would be if the finite sizes of the fillet weld and shell are ignored. In relation to the path of vertical loads, these pivoting locations have larger radial offsets at each flange than those for any of the postulated cracking scenarios (even for the case in which the cracking is in the shroud shell at the toe of the welds). Therefore, the resulting vertical flexibility of the shroud which is proportional in magnitude to the square value of these larger offsets renders conservative results.

The assumptions used to make the determination are:

1) All mechanical or other operations that affect the vertical deformations in the shroud, e.g., the pre tensioning of the core plate fasteners, take place prior to the pre tensioning of the Tie-rods.

2) The H8 weld, even if cracked will transmit the vertical loads exerted by the pressure differential on the shroud support (baffle) plate as a shell hinge-connection to the lower shroud and stilts (shroud support legs). In this analysis, the effect of this load transmittal is ignored leading to conservative results since the stilt stretching, due to the transmitted upward load, that tends to close the gap is ignored.

3) Loads and temperatures for the Normal operating condition are applied to
   a) the lower portion of the shroud severed from the upper part at weld H6;
   b) the upper portion of the shroud severed from the lower part at weld H6.

If the analysis shows that the resulting displacements of the edges at weld H6 of "a" and "b" indicate an overlap of the severed upper and lower parts at H6, it can be concluded that a gap will not open.

Because this analysis indicates an overlap (larger than 0.004 inch) of the free edges (resulting from severing the model at H6) in the normal operating condition, it is concluded that a gap will not open in this condition at a cracked H6 weld.

In the Upset Thermal case, the thermal strains from the temperature distribution cause a higher load in the tie rods than would exist under normal operating condition (in absence of seismic loads). This makes the normal operating condition the more critical case (more prone) relative to opening of a gap at a cracked H6. And, the thermal Upset condition becomes the more critical case (more prone) relative to over stressing the shroud due to the higher tie rod loads.

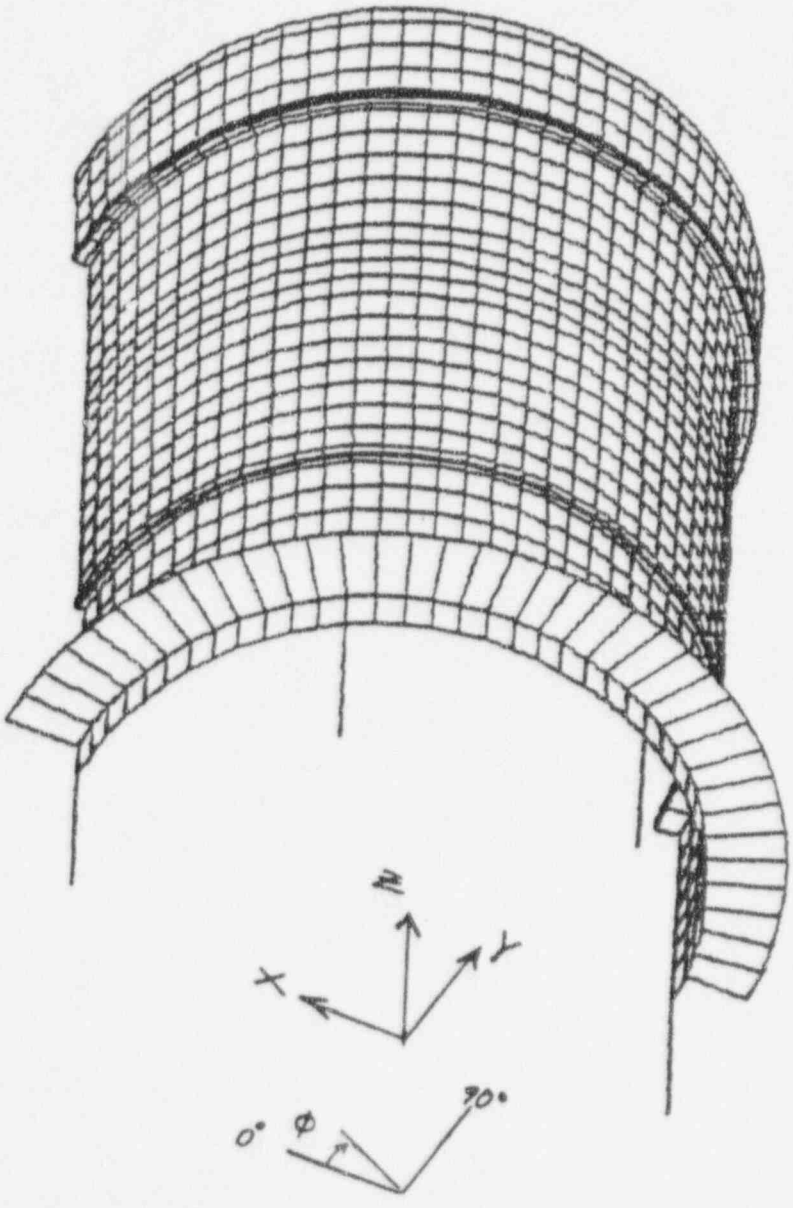

Figure 6.1 Shroud Finite Element Model

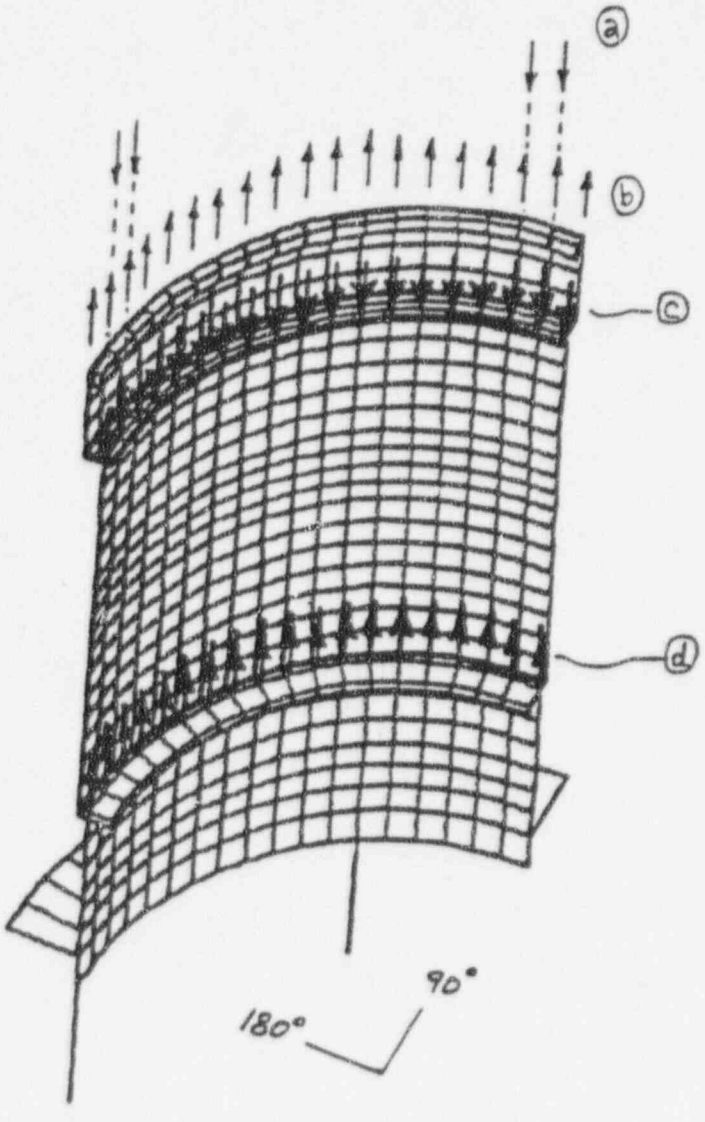

Symmetric Half of the model

Figure 6.2 Application of Tie Rod Forces (a) (at 4 nodes per tie rod), and Uniform Vertical Forces at the Shroud Head (b) (distributed equally among the nodes shown), Top Guide (c) (distributed equally among the nodes shown) and Core Plate (d) (distributed equally among the nodes shown) Flanges.

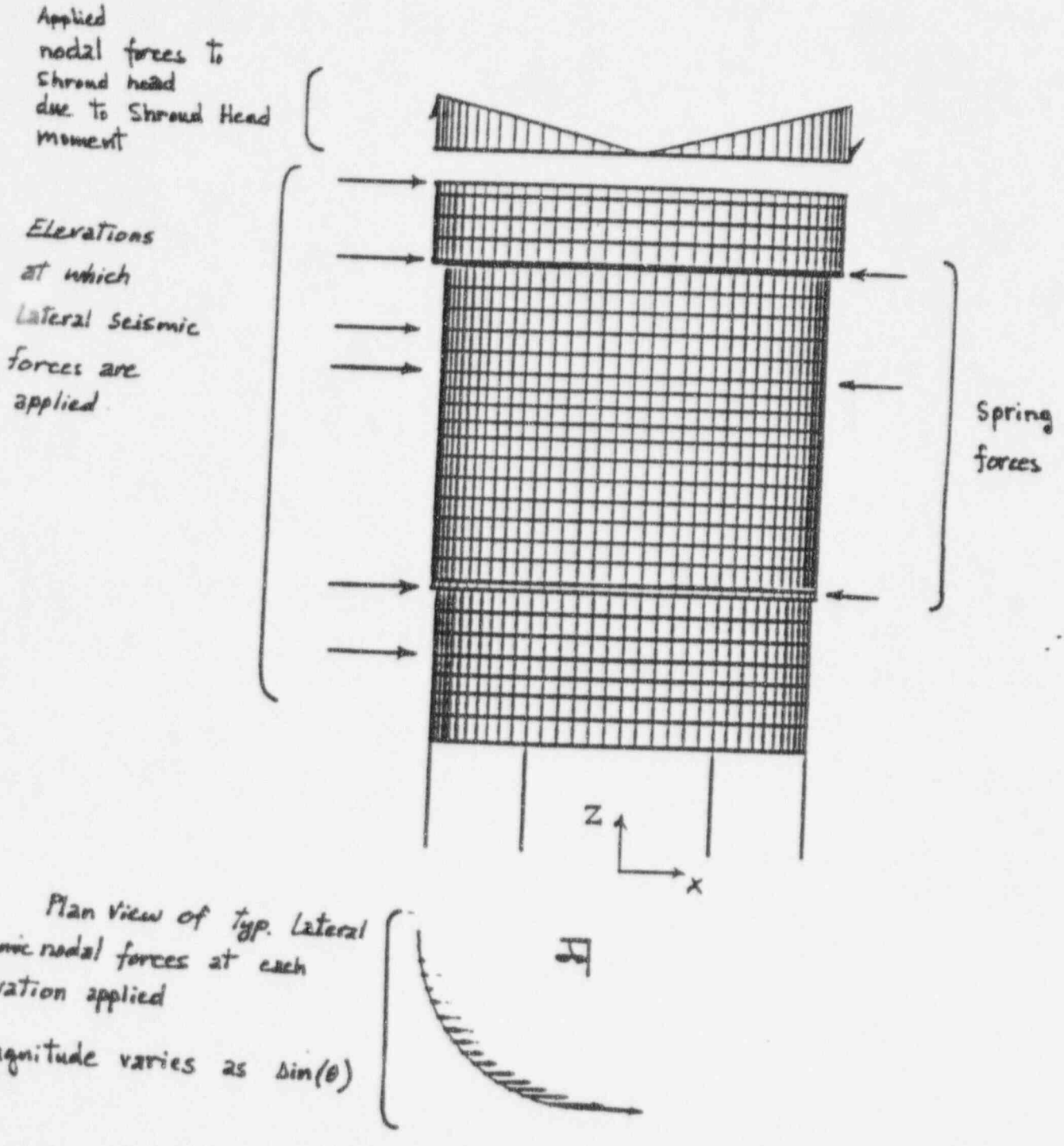

Figure 6.3 Application of Seismic Lateral Forces and Moment of Shroud Head

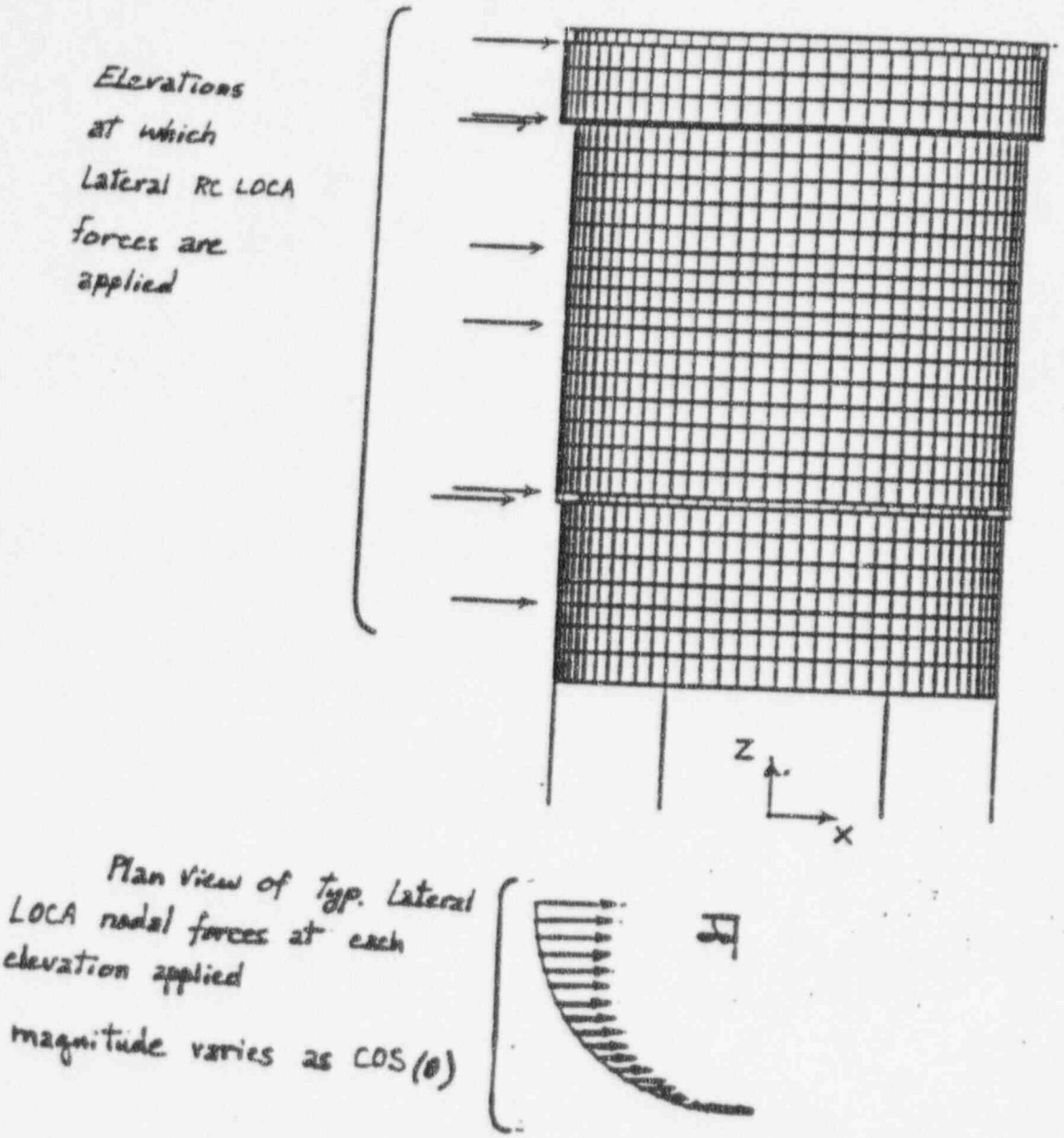

Figure 6.4 Application of RC LOCA Lateral Forces.

REFERENCES

1. ANSYS, General Purpose Finite Element Program, Version 4.4. Swanson Analysis Systems, Inc.

2. "Dresden 2 and 3 Shroud Stabilizer Hardware Design Specification", 25A5688, Rev.2.

3. ASME Boiler and Pressure Vessel Code, Section III, Appendices, 1989 Edition.

4. "Backup Calculations for RPV Stress Report for No. 25A5691, Dresden Units 2 and 3", GENE-771-77-1194, Rev. 2.

5. "Dresden 2 and 3 Shroud Repair Seismic Analysis", GENE-771-84-1194, Rev. 2.

6. "ComEd Technical Requirements Document for Dresden / Quad Cities Core Shroud Repair", NEC-12-4056.

7. "Dresden 2 and 3 RPV Stress Report", 25A5691, Rev.2.

8. "Project Instruction Shroud Repair For H1 Through H7 Welds For Commonwealth Edison Dresden Nuclear Power Station", GENE-771-80-1194, Rev. 1.

9. "Dresden Station Rebaselined UFSAR", Commonwealth Edison , 30 June 1993.

10. "Backup Calculations for Dresden Shroud Repair Shroud Stress Report for Commonwealth Edison Dresden Nuclear Power Station Units 2 & 3", GENE-771-82-1194, Rev. 1, May 1995.

Enclosure 7

GENE-771-82-1194, Revision 1

Backup Calculations for Dresden Shroud Repair Shroud Stress Report
Commonwealth Edison
Dresden Nuclear Power Station, Units 2 and 3